Statistical production and binding energy of hypernuclei

Nihal Buyukcizmeci

Selçuk University, Department of Physics, 42079, Konya, Turkey

in collaboration with A.S.Botvina, M. Bleicher, A. Ergun and R. Ogul

This study is supported by TUBITAK-114F328
and STSM of COST Action THOR CA15213.

COST THOR Working Group I & II & GDRI Meeting
COST Action CA15213 Instituto Superior Técnico, Universidade de Lisboa June 11-14, 2018

In nuclear reactions of high energy one can simultaneously produce a lot of hypernuclei after the capture of hyperons by nuclear residues. We consider statistical disintegration of such hypernuclear systems and the connection of fragment production with the binding energies of hyperons.

Buyukcizmeci N. et al, submitted to Phys. Rev C 2018, (**ArxiV: 1711.01159v2)**

Statistical approach in nuclear reactions: conception of equilibrium

Intermediate energy collisions

Preequlibrium emission + equilibration

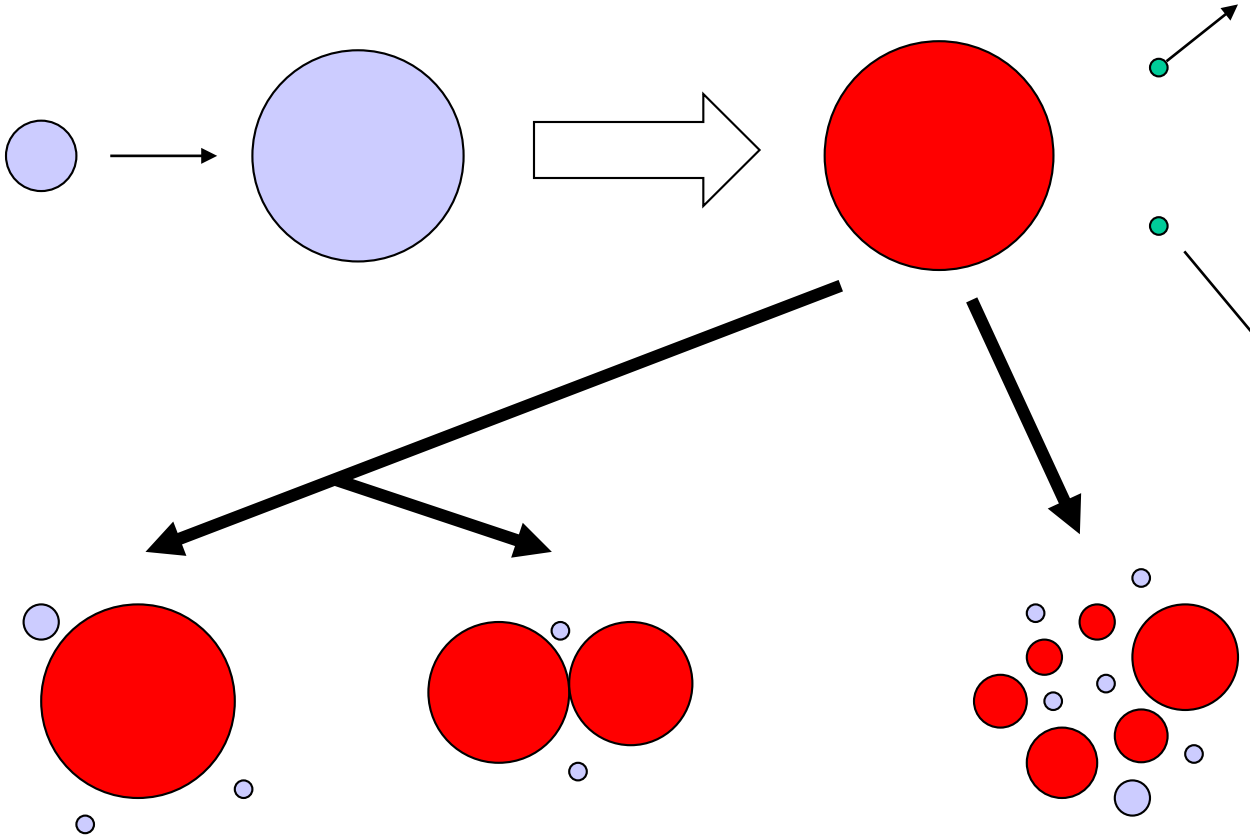

N.Bohr (1936)

Compound-nucleus decay channels (sequential evaporation or fission) dominate at low excitation energy of thermal sources $E^{*}<2$-3 MeV/nucl

starting 1980-th :

At high excitation energy $E^{*}>3$-4 MeV/nucl there is a simultaneous break-up into many fragments

evaporation fission multifragmentation

V.Weisskopf (1937) N.Bohr, J.Wheeler (1939) Bondorf et al. (1995) SMM

Multifragmentation in intermediate and high energy nuclear reactions

Experimentally established:

1) few stages of reactions leading to multifragmentation,
2) short time ~100fm/c for primary fragment production,
3) freeze-out density is around $0.1\rho_0$,
4) high degree of equilibration at the freeze-out,
5) primary fragments are hot.

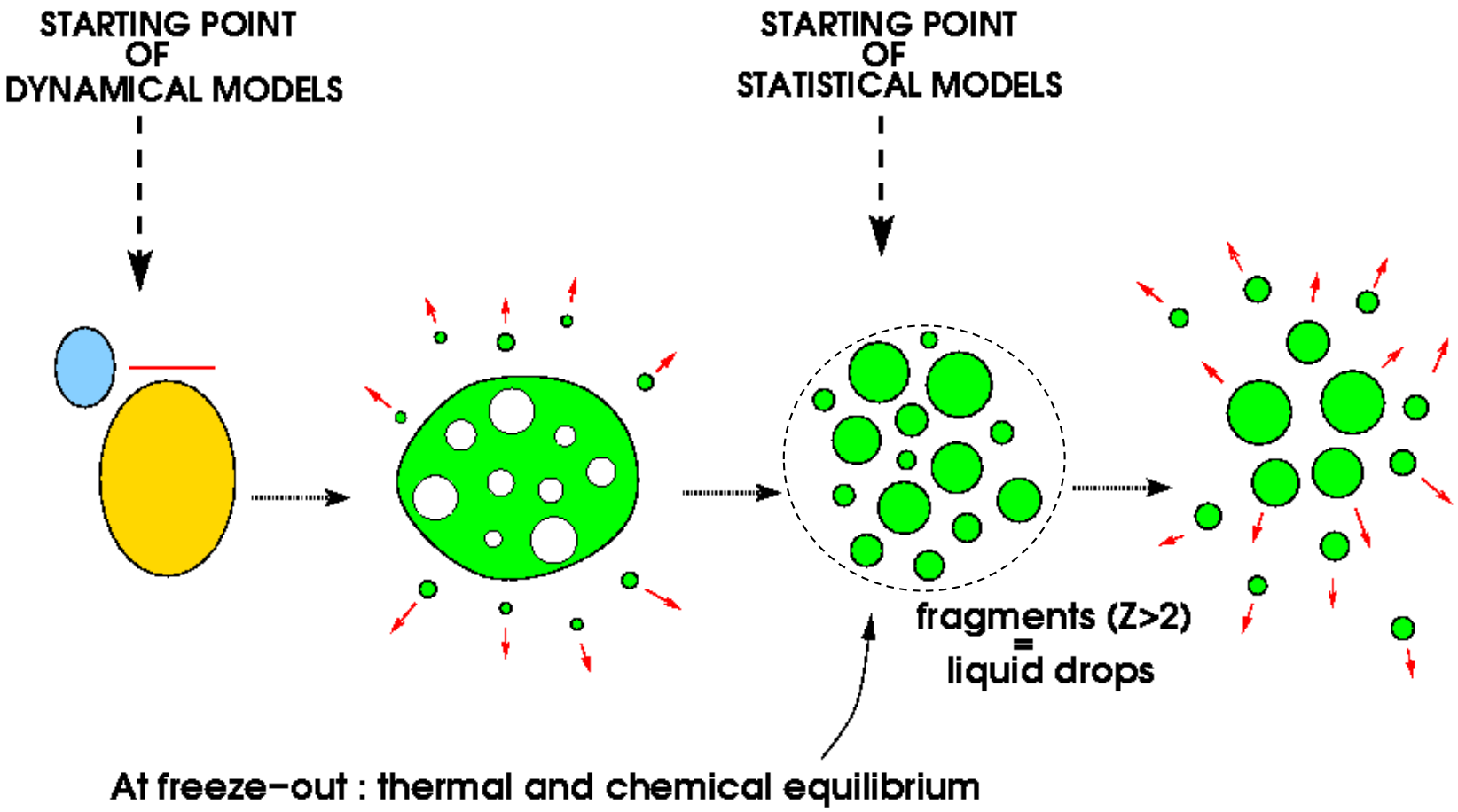

ALADIN data

GSI

multifragmentation of relativistic projectiles

A.S.Botvina et al.,
Nucl.Phys. A584(1995)737

comparison with SMM (statistical multifragmentation model)

Statistical equilibrium has been reached in these reactions

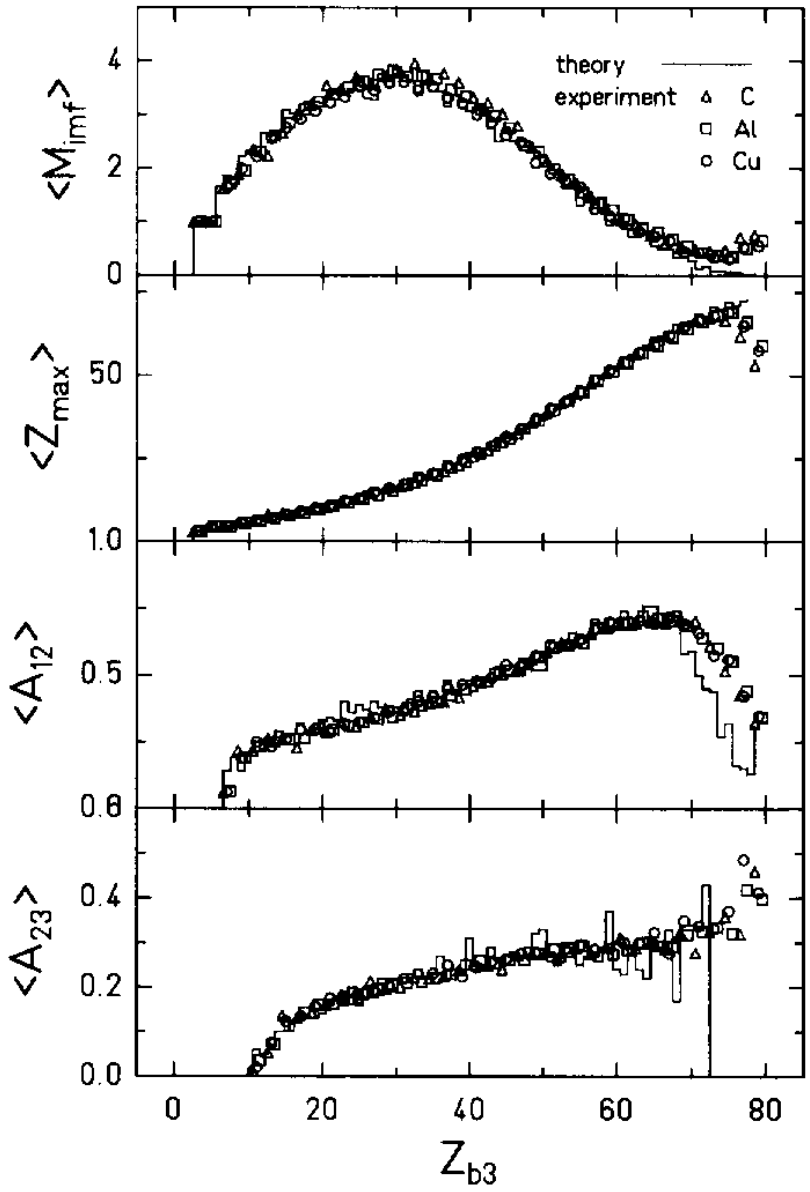

Fig. 7. Mean values of the multiplicity of intermediate-mass fragments $\langle M_{\mathrm{imf}} \rangle$, the maximum fragment charge $\langle Z_{\mathrm{max}} \rangle$ and of the first and second fragment asymmetries $\langle A_{12} \rangle$ and $\langle A_{23} \rangle$ versus the bound charge Z_{b3} for the reactions ^{197}Au on C (triangles), Al (squares) and Cu (circles) at $E/A = 600$ MeV. A threshold of $Z \geqslant 3$ was required for all observables. The results calculated for ^{197}Au on Cu are given by the histogram.

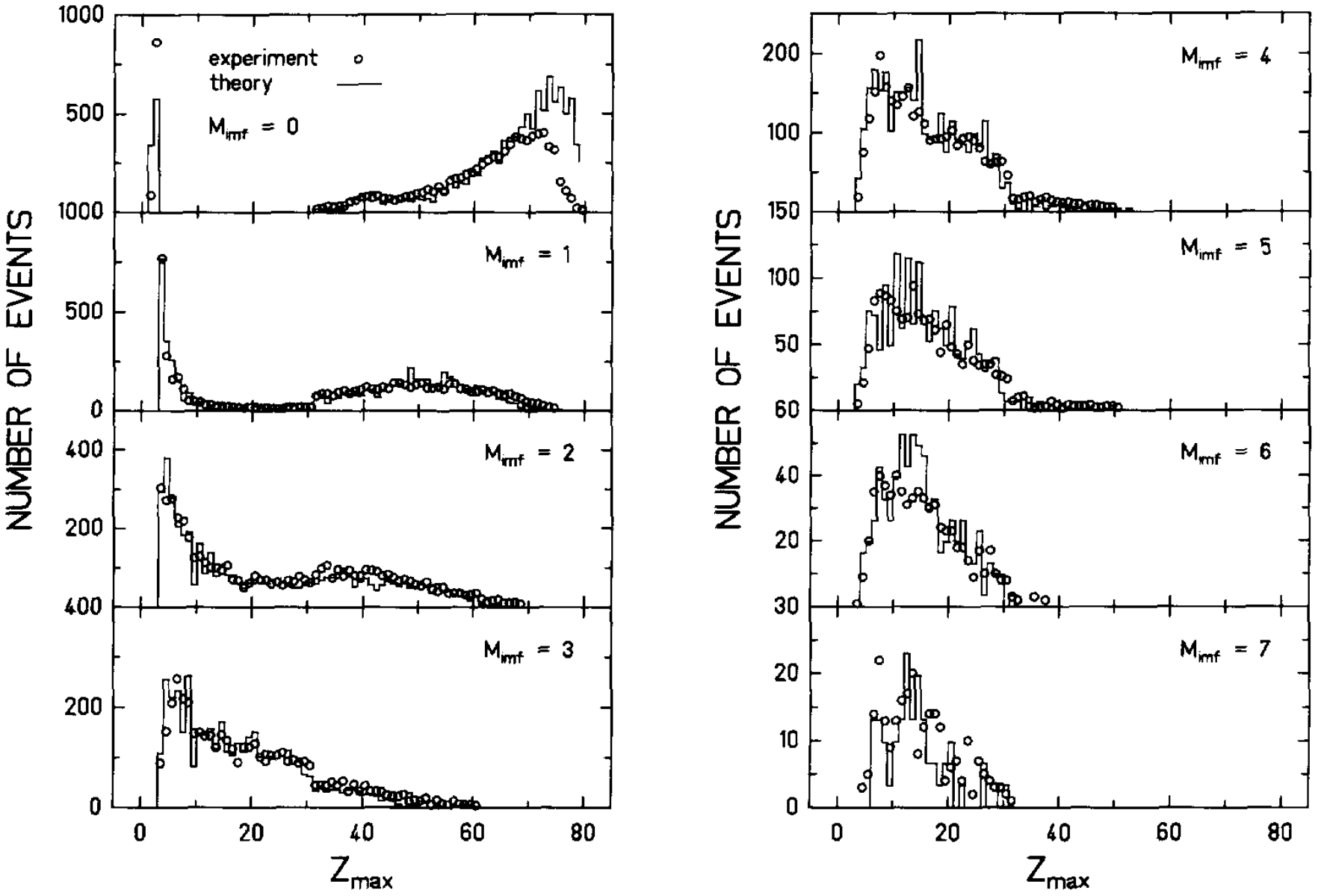

Fig. 10. Distributions of of the atomic number Z_{max} of the largest fragment within an event for the indicated values of M_{imf} for the reaction ^{197}Au on Cu at $E/A = 600$ MeV. The measured data and the calculated results are represented by the open circles and by the histogram, respectively.

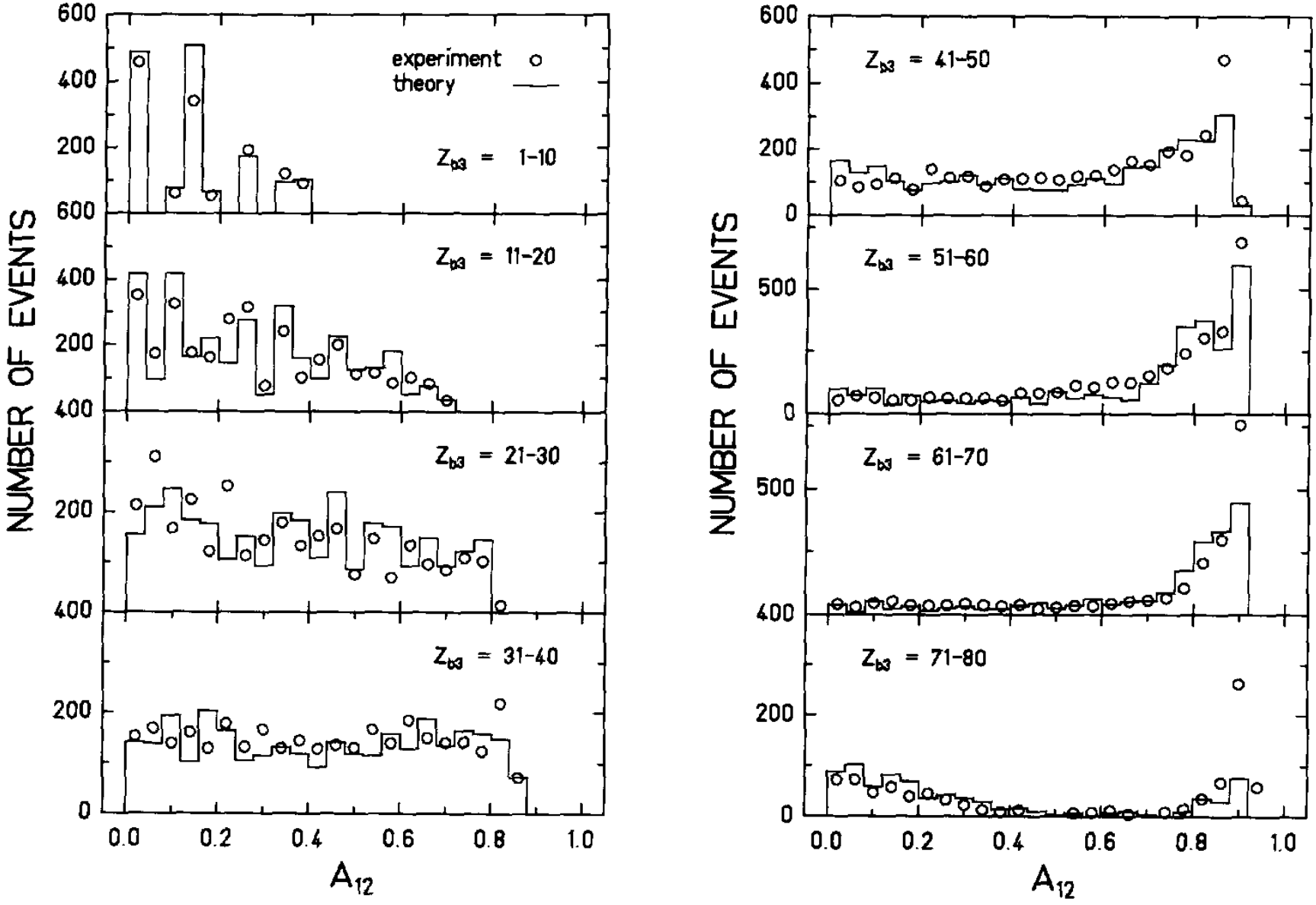

Fig. 12. Distributions of the charge asymmetry A_{12} of the two largest fragments for the indicated bins of Z_{b3} for the reaction ^{197}Au on Cu at E/A = 600 MeV. Events with at least two fragments with $Z \geqslant 3$ have been selected. The measured data and the calculated results are represented by the open circles and by the histogram, respectively.

R.Ogul et al. PRC **83,** 024608 (2011) **ALADIN@GSI**

Isospin-dependent multifragmentation of relativistic projectiles

124,107-**Sn**, 124-**La** (600 A MeV) + **Sn** → projectile (multi-)fragmentation

Very good description is obtained within Statistical Multifragmentation Model, including fragment charge yields, isotope yileds, various fragment correlations.

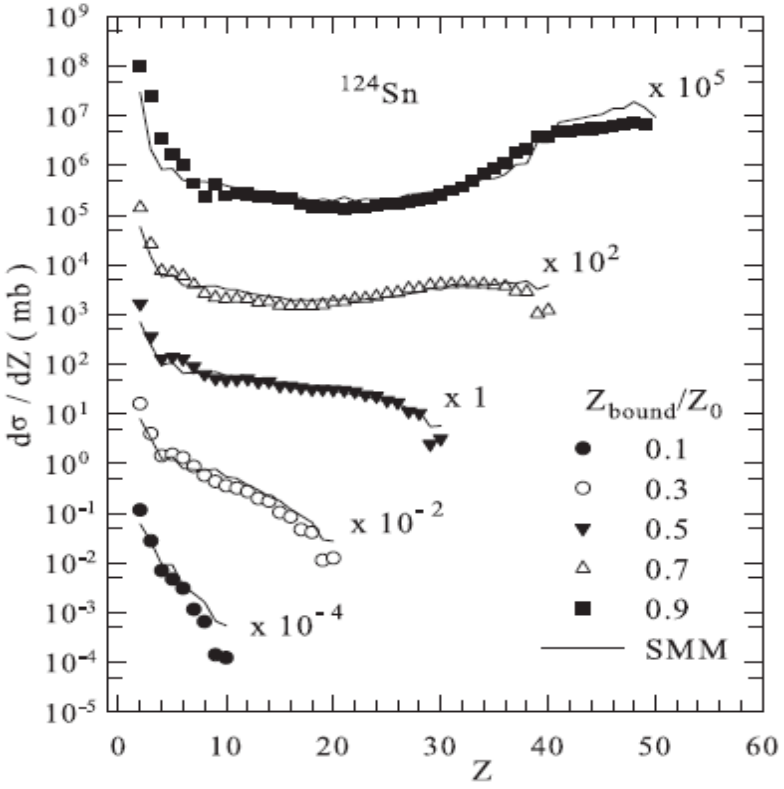

Statistical (chemical) equilibrium is established at break-up of hot projectile residues ! In the case of strangeness admixture we expect it too !

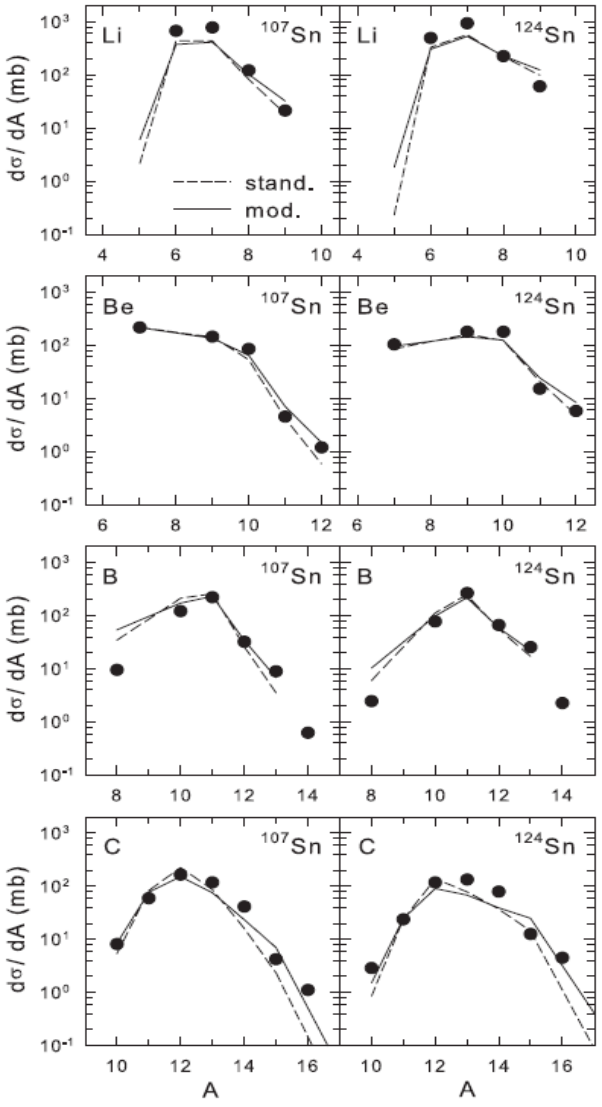

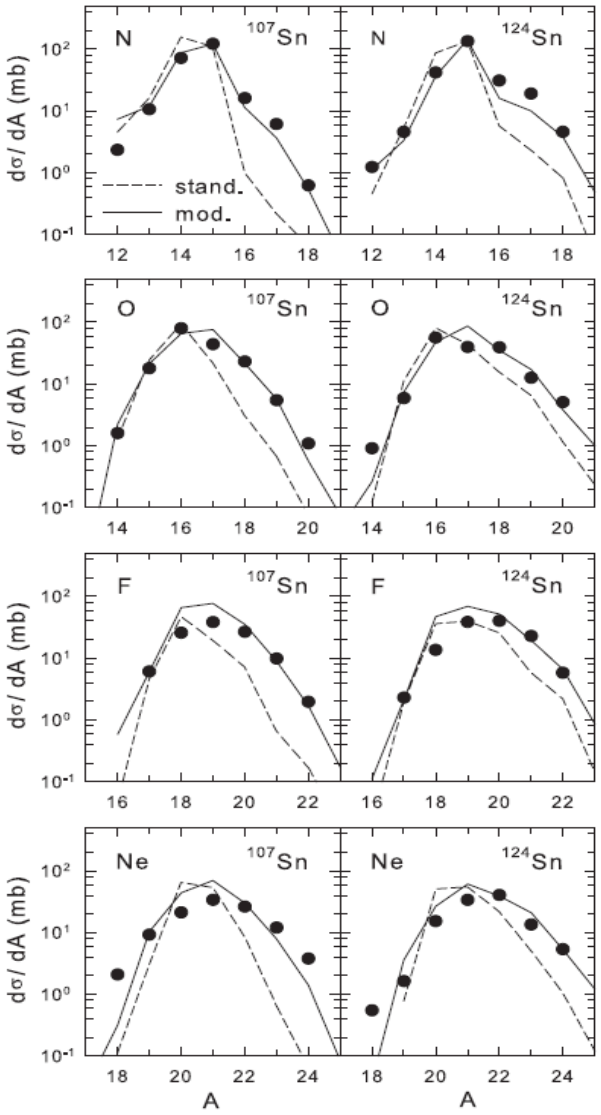

FRS data @ GSI

FRS projectile fragmentation of two symetric systems ^{124}Sn + ^{124}Sn and ^{112}Sn + ^{112}Sn at an incident beam energy of 1 A GeV measured with high-resolution magnetic spectrometer FRS.
(V. Föhr, et al., Phys. Rev. **C 84**, (2011) 054605)

Z interval	^{112}Sn γ(MeV)	^{124}Sn γ (MeV)
10-17	16	16
18-25	19	18
26-31	21	20
32-37	23	19
38-45	25	18

Experimental data are well reproduced with statistical calculations in the SMM–ensemble .
To reproduce the FRS data symmetry energy term is reduced as shown in the table.
We have also found a decreasing trend of the symmetry energy with increasing charge number, for the neutron-rich heavy fragments resulting from ^{124}Sn projectile.
H. Imal, A.Ergun, N. Buyukcizmeci, R.Ogul, A.S. Botvina, W. Trautmann, C **91**, 034605 (2015)

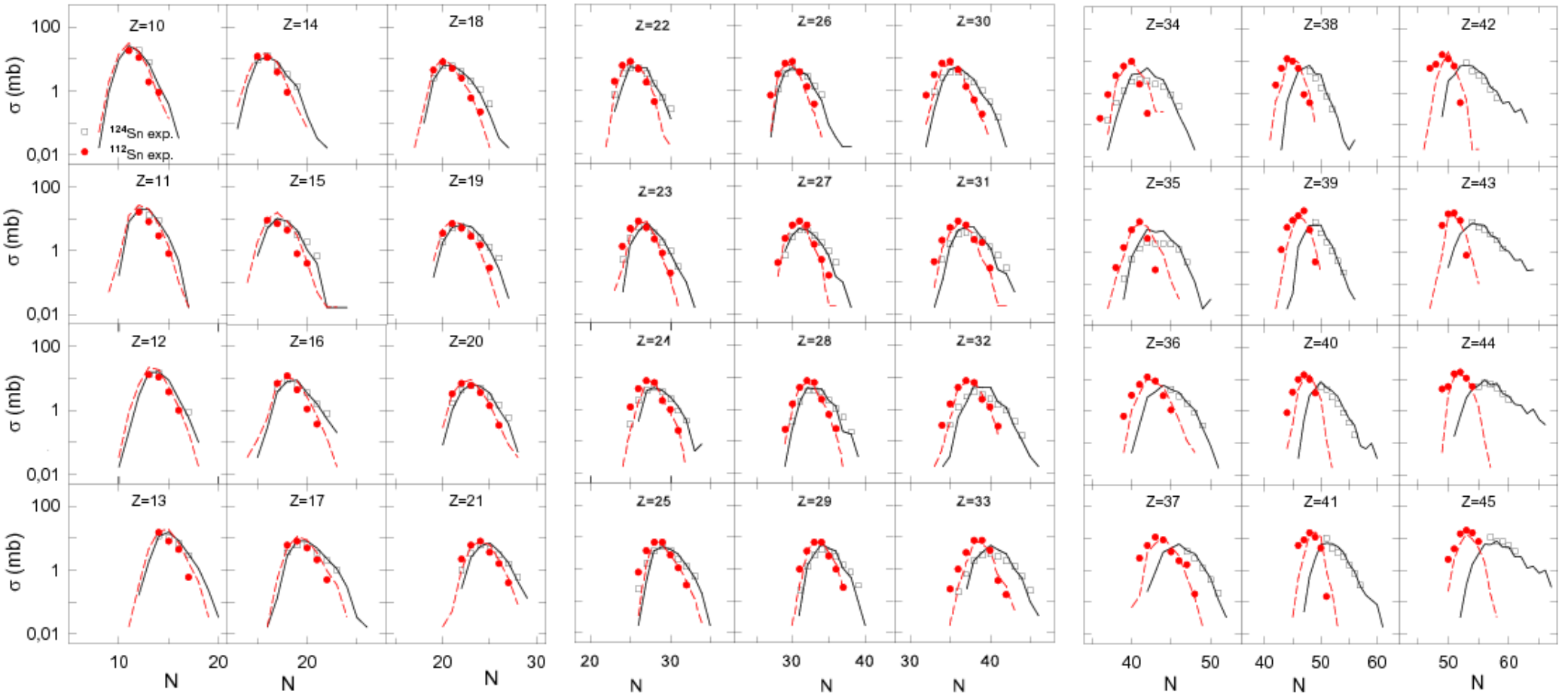

Discovery of a Strange nucleus: Hypernucleus

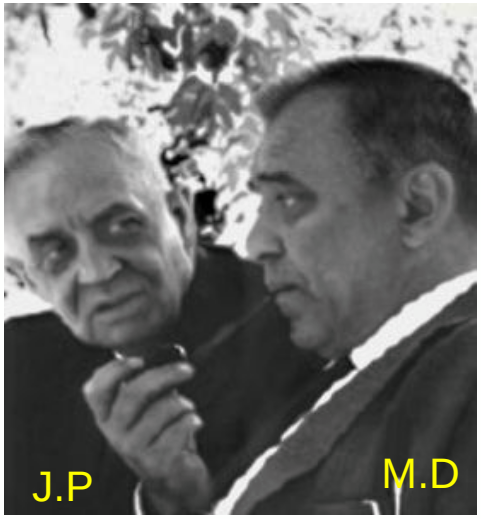

M. Danysz and J. Pniewski, Philos. Mag. 44 (1953) 348

First-hypernucleus was observed in a stack of photographic emulsions exposed to cosmic rays at about 26 k above the ground.

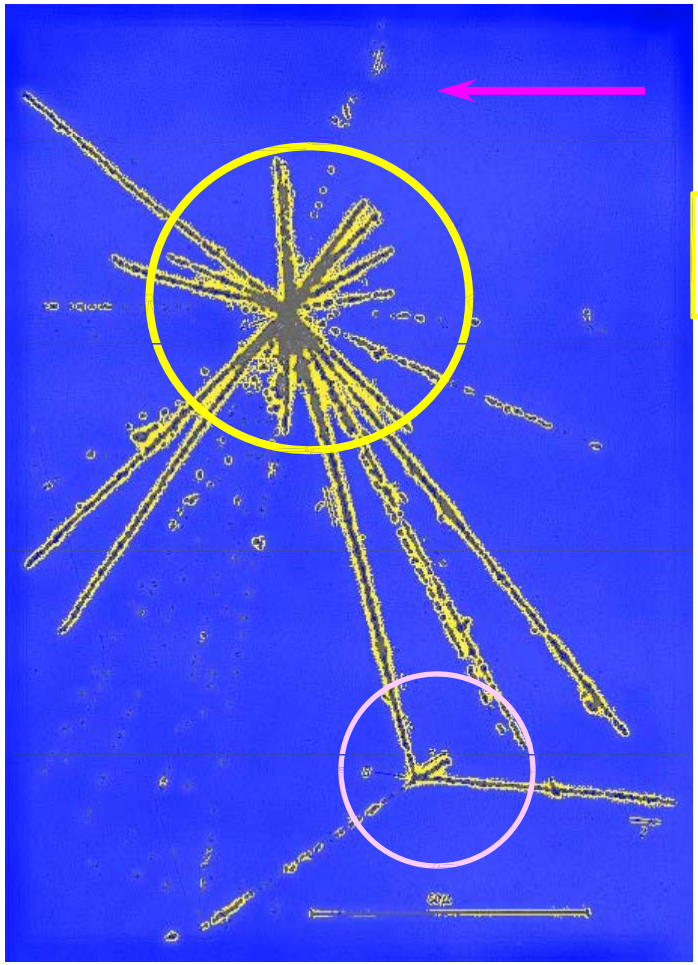

Incoming high energy proton from cosmic ray

colliding with a nucleus of the emulsion, breaks it in several fragments forming a star.

All nuclear fragments stop in the emulsion after a short path

From the first star, 21 Tracks => $9\alpha + 11H + 1\ {}_{\Lambda}X$

The fragment ${}_{\Lambda}X$ disintegrates later , makes the bottom star. Time taken ~ 10^{-12} sec (typical for weak decay)

This particular nuclear fragment, and the others obtained afterwards in similar conditions, were called **hyperfragments or hypernuclei.**

Hyperons: Baryons with Strangeness

Lambda

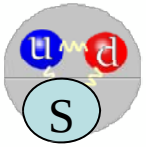

$\Lambda^0=(uds)$

$m(\Lambda^0)$ = 1115.683 +/- 0.006 MeV

S = - 1

Quark	Symbol	charge (e)	Strangeness (S)
Up	(u)	2/3	0
Down	(d)	-1/3	0
Strange	(s)	-1/3	-1
Charm	(c)	2/3	0
Bottom	(b)	-1/3	0
Top	(t)	2/3	0

lifetimes of ~1×10^{-10} s

with the exception of Σ^0

whose lifetime is

shorter than 1×10^{-19} s

Sigma

$\Sigma^0=(uds)$

$m(\Sigma^0)$ = 1192.642 +/- 0.024 MeV

S = - 1

$\Sigma^-=(dds)$

$m(\Sigma^-)$ = 1197.449 +/- 0.030 MeV

S = - 1

$\Sigma^+(uus)$

$m(\Sigma^+)$ =1189.37 +/- 0.07 MeV

S = - 1

Cascade or Xi

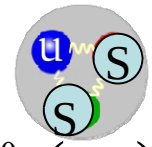

$\Xi^0=(uss)$

$m(\Xi^0)$ = 1314.86 +/- 0.2 MeV

S = - 2

$\Xi^-=(dss)$

$m(\Xi^-)$ = 1321.71 +/- 0.07 MeV

S = - 2

Omega

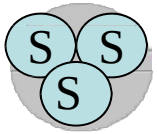

$\Omega^-=(sss)$

$m(\Omega^-)$ = 1672.45 +/- 0.29 MeV

S = - 3

lifetime of ~ 8.2×10^{-11} s

Why Study Hypernuclei?

A hyperon can be put deep inside a nucleus => **No Pauli blocking** by the nucleons.

Hence, it can be used as a sensitive probe of the nuclear interior.

- NN interaction ✂ Well known from elastic scattering data
- YN, YY interaction ✂ Very little data

(short lifetime (ct < 10 cm), yield low)

- unified understanding of NN, YN and YY interactions

❖**Production of nuclei-beyond drip lines**

❖**Production of exotic multi-strange nuclei – may be without any neutrons and protons!**

HYPERNUCLEI & ASTROPHYSICS

❖**Hyperons** may appear at the high density core of the neutron star

❖At a density of four to five times that of nuclear matter saturation density ρ_0, a neutron star can become a hyperon star.

❖Theoretical models predict that the presence of strange baryons in neutron stars strongly affect their properties, like size, mass etc.

❖The effect strongly depends upon the interactions of strange baryons which is still very poorly known!

More experimental data needed to constrain theoretical models.

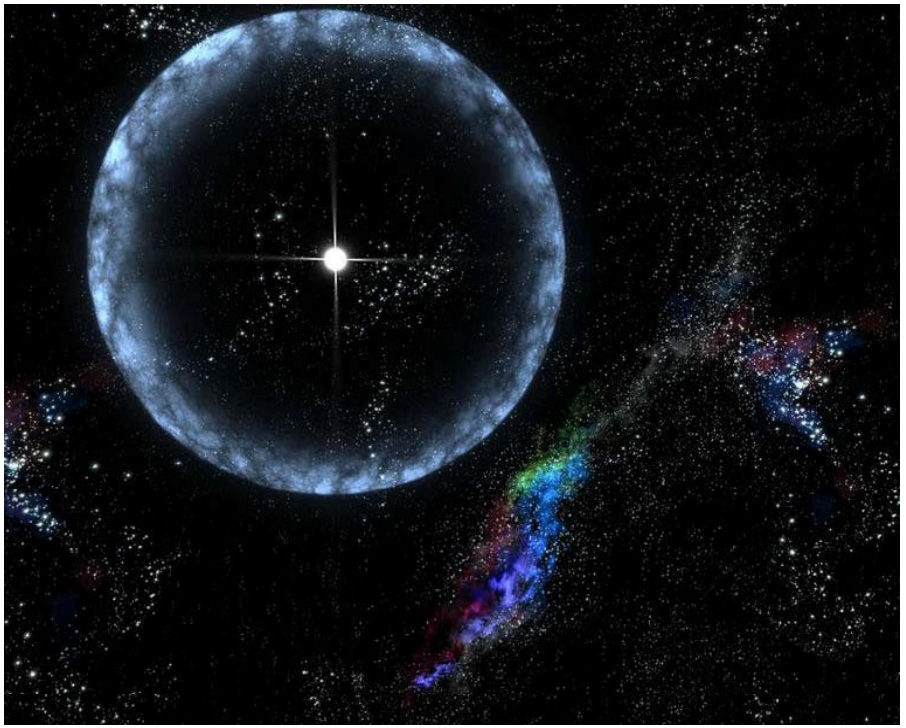

http://en.wikipedia.org/wiki/Neutron_star

J. Schaffner and I.N.Mishustin,
"Hyperon-rich matter in neutron stars".
Phys. Rev.C 53 (1996) 1416-1429.

Nuclear reactions: production mechanisms for hypernuclei

Traditional way for production of hypernuclei:
Conversion of Nucleons into Hyperons
by using hadron and electron beams

(CERN, BNL, KEK, CEBAF, DAΦNE, JPARC, MAMI, ...)

Advantages: rather precise determination of masses
(e.g., via the missing mass spectroscopy) :
good for nuclear structure studies !

Disadvantages: very limited range of nuclei in A and Z can beinvestsigated; the phase space of the reaction is narrow (since hypernuclei are produced in ground and slightly excited states), so production probability is low; it is difficult to produce multi-strange nuclei.

What reactions can be used to produce exotic strange nuclei and nuclei with many hyperons ?

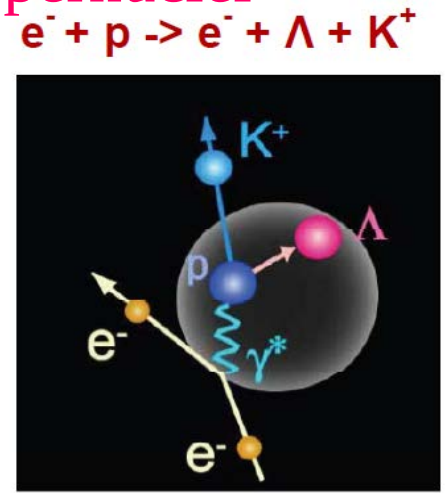

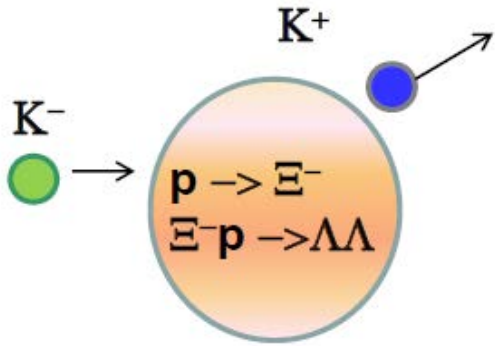

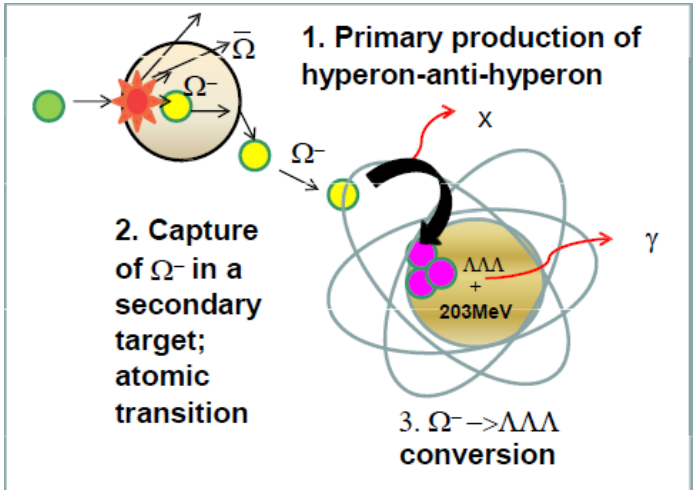

A.S.Botvina and J.Pochodzalla, Phys. Rev.C76 (2007) 024909

Generalization of the statistical de-excitation model for nuclei with Lambda hyperons

In these reactions we expect analogy with

multifragmentation in intermediate and high energy nuclear reactions

+ nuclear matter with strangeness

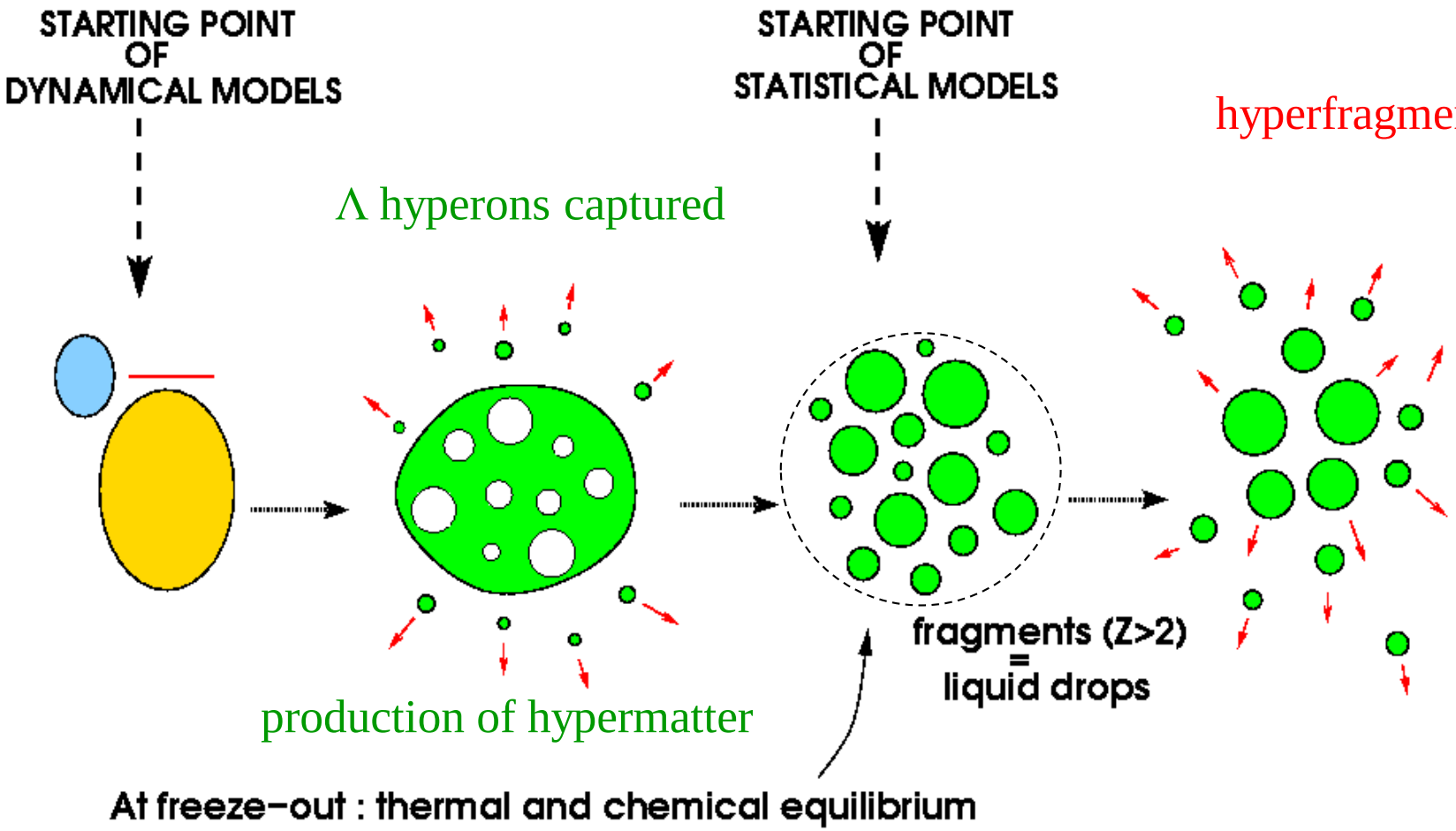

Statistical approach for fragmentation of hyper-matter

$$Y_{AZH} = g_{AZH} V_f \frac{A^{3/2}}{\lambda_T^3} \exp\left[-\frac{1}{T}\left(F_{AZH} - \mu_{AZH}\right)\right]$$

$$\mu_{AZH} = A\mu + Z\nu + H\xi$$

mean yield of fragments with mass number ***A***, charge ***Z***, and **Λ**-hyperon number ***H***

$$F_{AZH}(T,V) = F_A^B + F_A^S + F_{AZH}^{sym} + F_{AZ}^C + F_{AH}^{hyp}$$

liquid-drop description of fragments: bulk, surface, symmetry, Coulomb (as in Wigner-Seitz approximation), and hyper energy contributions
J.Bondorf et al., Phys. Rep. **257** (1995) 133

$$F_A^B(T) = \left(-w_0 - \frac{T^2}{\varepsilon_0}\right) A \quad ,$$

$$F_A^S(T) = \beta_0 \left(\frac{T_c^2 - T^2}{T_c^2 + T^2}\right)^{5/4} A^{2/3} \quad ,$$

parameters ≈ Bethe-Weizsäcker formula:

$w_0 = 16$ MeV, $\beta_0 = 18$ MeV, $T_c = 18$ MeV

$$F_{AZH}^{sym} = \gamma \frac{(A - H - 2Z)^2}{A - H} \quad ,$$

$\gamma = 25$ MeV $\varepsilon_0 \approx 16$ MeV

$$\sum_{AZH} A Y_{AZH} = A_0, \sum_{AZH} Z Y_{AZH} = Z_0, \sum_{AZH} H Y_{AZH} = H_0.$$

chemical potentials are from mass, charge and *H*yperon number conservations

$$F_{AH}^{hyp} = E_{sam}^{hyp} = H \cdot (-10.68 + 48.7/(A^{2/3})).$$

-- C.Samanta et al. J. Phys. G: 32 (2006) 363
(motivated: single **Λ** in potential well)

$$F_{AH}^{hyp} = (H/A) \cdot (-10.68A + 21.27A^{2/3}).$$

-- liquid-drop description of hyper-matter

A.S.Botvina and J.Pochodzalla, Phys. Rev.C76 (2007) 024909

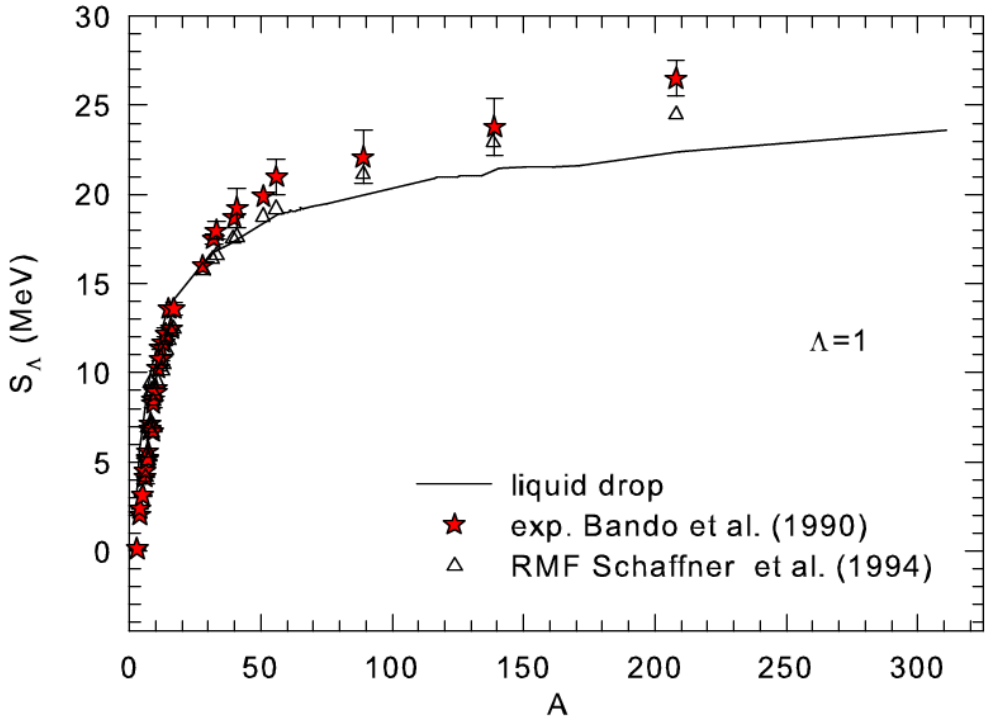

Separation energy

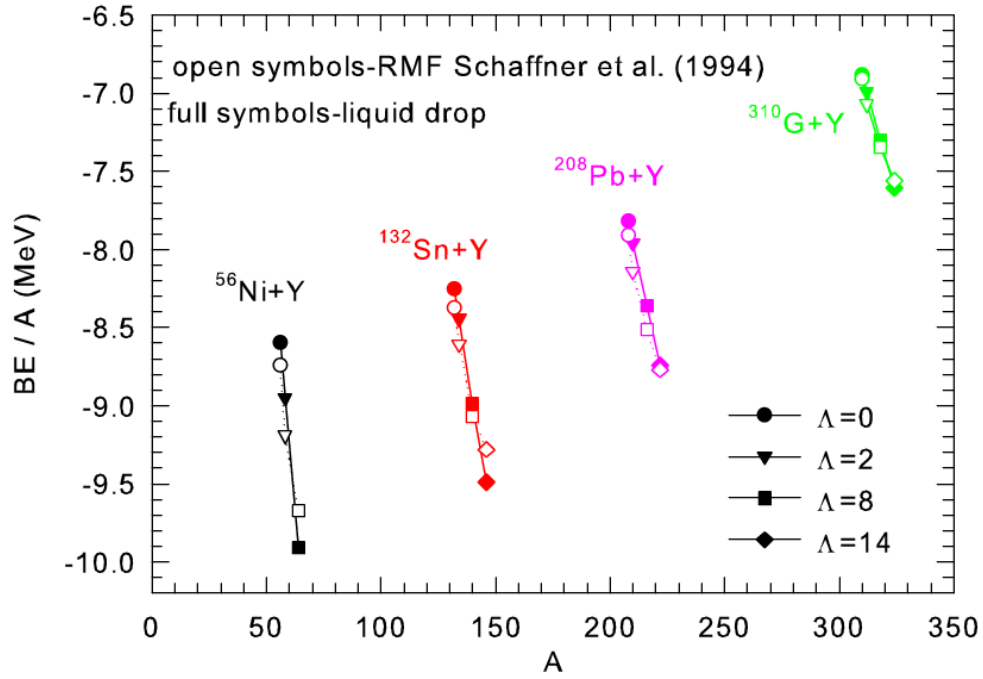

Binding energy

liquid-drop approximation

N.Buyukcizmeci et al., PRC88 (2013) 014611

Break-up of excited hyper-residues

Normal nuclei + hypernuclei can be formed via evaporation, fission and multifragmentation processes.

Liquid-gas type phase transition in hyper-matter is expected at subnuclear densities.

Very broad distributions of nuclei similar to ones in normal nuclear matter. At moderate temperatures hyperons concentrate in large species

Important: formed hypernuclei can reach beyond traditional neutron and proton drip-lines

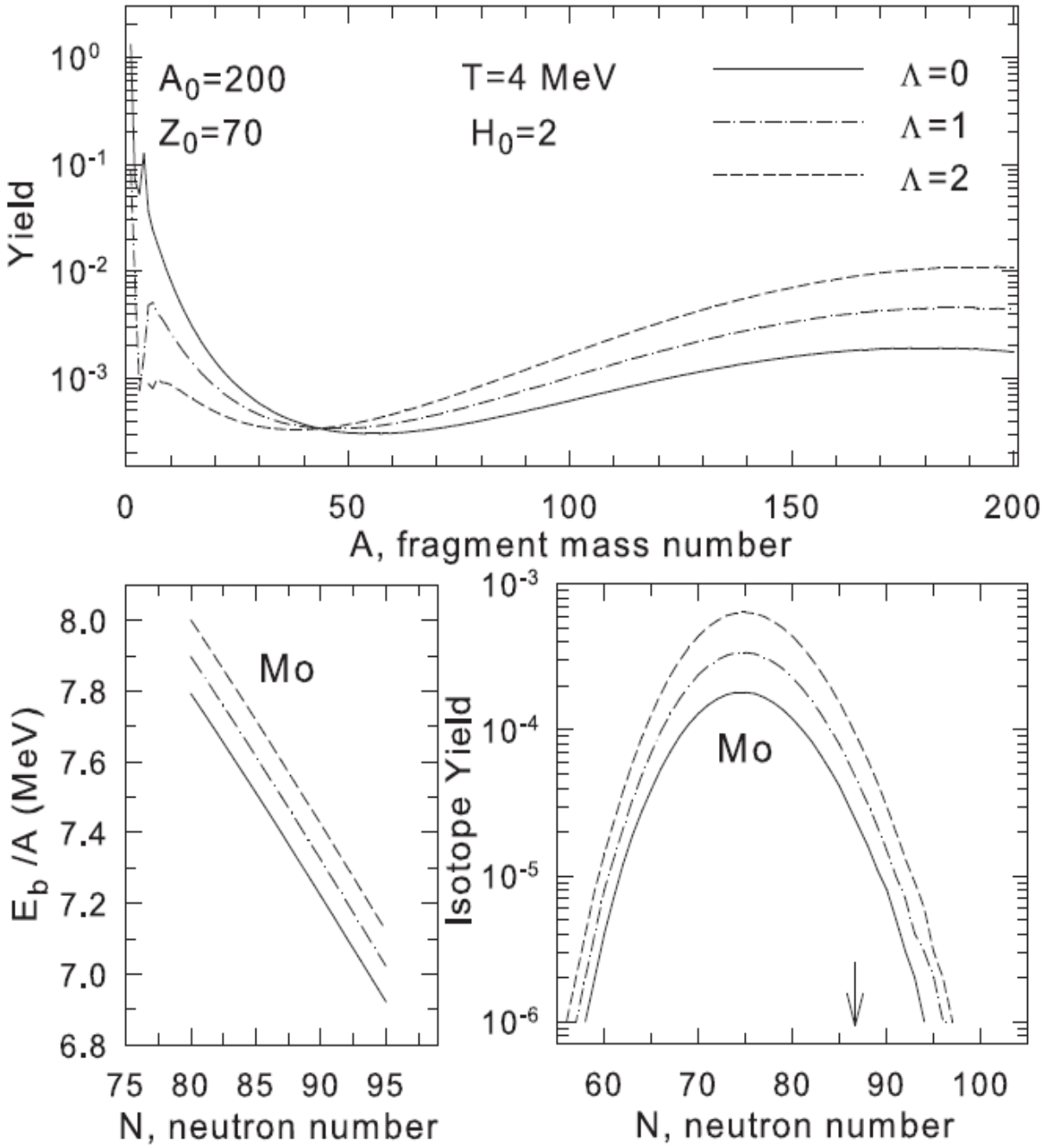

N.Buyukcizmeci et al., PRC88 (2013) 014611

Double ratio method for hypernuclei

ArxiV: 1711.01159v2

Grand

Canonical approximations leads to the following average yields of individual fragments with the mass (baryon) number A, charge Z, and the Λ-hyperon number H:

$$Y_{\mathrm{A,Z,H}} = g_{\mathrm{A,Z,H}} \cdot V_f \frac{A^{3/2}}{\lambda_T^3} \exp\left[-\frac{1}{T}\left(F_{A,Z,H} - \mu_{AZH}\right)\right],$$
$$\mu_{AZH} = A\mu + Z\nu + H\xi. \qquad (1)$$

Here T is the temperature, $F_{A,Z,H}$ is the internal free energies of these fragments, V_f is the free volume available for the translation motion of the fragments, $g_{\mathrm{A,Z,H}}$ is the spin degeneracy factor of species (A, Z, H), $\lambda_T = \left(2\pi\hbar^2/m_N T\right)^{1/2}$ is the baryon thermal wavelength, m_N is the average baryon mass. The chemical potentials μ, ν, and ξ are responsible for the mass (baryon) number, charge, and strangeness conservation in the system, and they can be numerically found from the corresponding conservation

$$F_{A,Z,H} = F_A^B + F_A^S + F_{AZH}^{\mathrm{sym}} + F_{AZ}^C + F_{AH}^{\mathrm{hyp}}$$

$$F_{AH}^{\mathrm{hyp}} = (H/A) \cdot (-10.68A + 21.27A^{2/3}) MeV$$

It is convenient to rewrite the above formulas in order to show separately the binding energy $E_A^{\rm bh}$ of one hyperon at the temperature T inside a hypernucleus with A, Z, H :

$$E_A^{\rm bh} = F_{A,Z,H} - F_{A-1,Z,H-1} \ . \tag{4}$$

Since Λ-hyperon is usually bound, this value is negative. Then the yield of hypernuclei with an additional Λ hyperon can be recursively written by using the former yields:

$$Y_{\rm A,Z,H} = Y_{\rm A-1,Z,H-1} \cdot C_{\rm A,Z,H} \cdot \exp\left[-\frac{1}{T}\left(E_A^{\rm bh} - \mu - \xi\right)\right], \tag{5}$$

where $C_{\rm A,Z,H} = (g_{\rm A,Z,H}/g_{\rm A-1,Z,H-1}) \cdot (A^{3/2}/(A-1)^{3/2})$ depends mainly on the ratio of the spin factors of A, Z, H and $A-1, Z, H-1$ nuclei, and very weakly (especially for large nuclei) on A. Since in the liquid-drop approximation we assume that the fragments with $A > 4$ are excited and do populate many states (above the ground) according to the given temperature dependence of the free energy, then we take $g_{\rm A,Z,H} = 1$. Within SMM

We suggest the following receipt for obtaining information on the binding energies of hyperons inside nuclei. Let us take two hyper-nuclei with different masses, (A_1, Z_1, H) and (A_2, Z_2, H), together with nuclei which differ from them only by one Λ hyperon. When we consider the double ratio (DR) of $Y_{\mathrm{A_1,Z_1,H}}/Y_{\mathrm{A_1-1,Z_1,H-1}}$ to $Y_{\mathrm{A_2,Z_2,H}}/Y_{\mathrm{A_2-1,Z_2,H-1}}$ we obtain from the above formulae

$$DR_{A_1A_2} = \frac{Y_{\mathrm{A_1,Z_1,H}}/Y_{\mathrm{A_1-1,Z_1,H-1}}}{Y_{\mathrm{A_2,Z_2,H}}/Y_{\mathrm{A_2-1,Z_2,H-1}}} = \alpha_{A_1A_2}\exp\left[-\frac{1}{T}\left(\Delta E^{\mathrm{bh}}_{A_1A_2}\right)\right], \tag{6}$$

where

$$\Delta E^{\mathrm{bh}}_{A_1A_2} = E^{\mathrm{bh}}_{A_1} - E^{\mathrm{bh}}_{A_2}, \tag{7}$$

and the ratio of the C-coefficients we denote as

$$\alpha_{A_1A_2} = C_{\mathrm{A_1,Z_1,H}}/C_{\mathrm{A_2,Z_2,H}}\ . \tag{8}$$

As one can see from eq.(6), the logarithm of the double ratio is directly proportional to the difference of the hyperon binding energies in A_1 and A_2 hypernuclei, $\Delta E^{\mathrm{bh}}_{A_1A_2}$, divided by temperature. Therefore, we can finally rewrite the relation between the hypernuclei yield ratios and the hyperon binding energies as

$$\Delta E^{\mathrm{bh}}_{A_1A_2} = T\cdot\left[ln(\alpha_{A_1A_2}) - ln(DR_{A_1A_2})\right]. \tag{9}$$

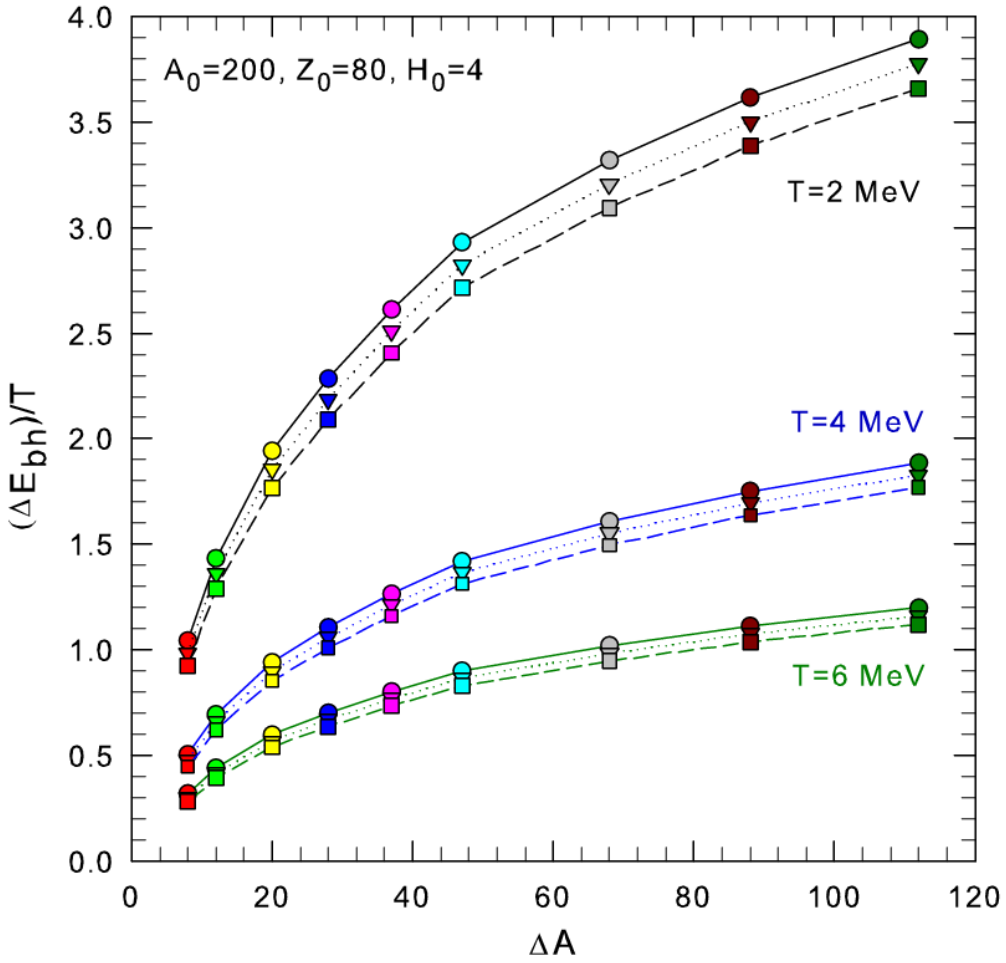

FIG. 1: (Color online) The difference of binding energies of hyperons in nuclei ($\Delta E_{\rm bh}$) divided by the temperature T versus the mass number difference of these nuclei ΔA as calculated with the statistical model at different temperatures typical for multifragmentation reactions. Baryon composition and temperatures (for groups of curves) of the initial system are given in the figure. The results for used isotopes (see the text) are demonstrated by different color symbols connected with lines: Circles (solid lines) are for single hypernuclei, inverse triangles (dotted lines) are for double hypernuclei, squares (dashed lines) are for triple hypernuclei.

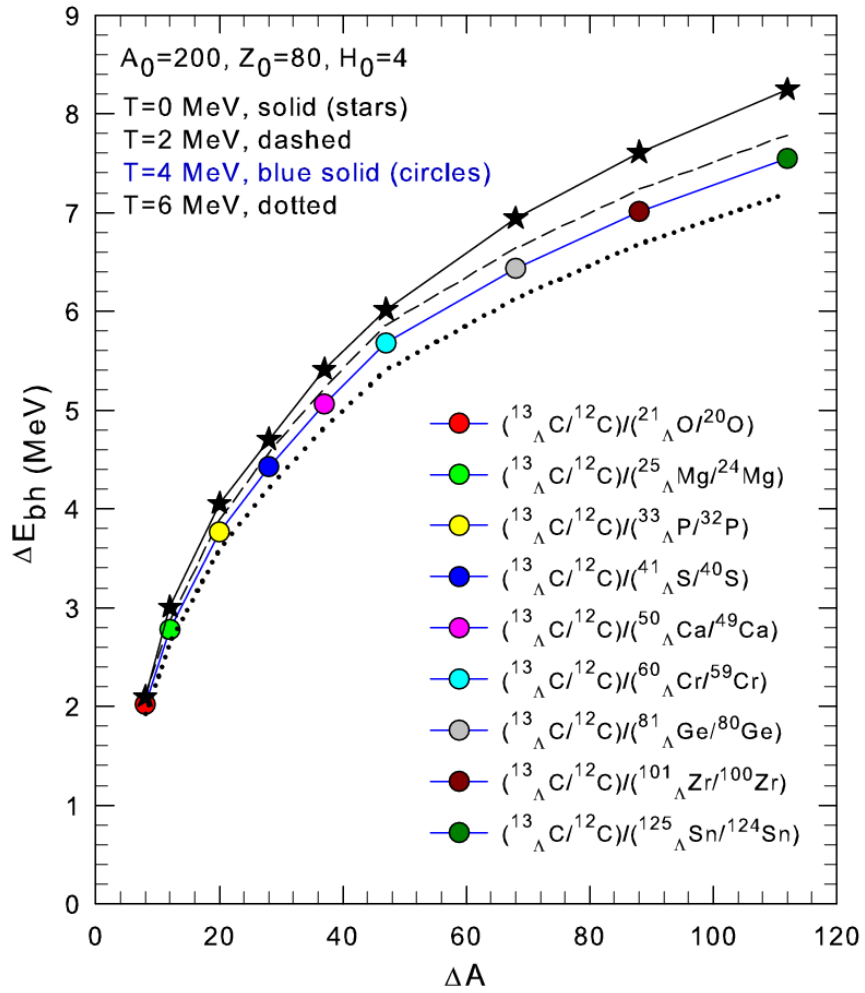

FIG. 2: (Color online) The modelled difference of binding energies of hyperons in nuclei ($\Delta E_{\rm bh}$) versus the mass number difference of these nuclei ΔA for single hypernuclei. The statistical calculations are performed involving the double ratio yields shown in the figure, and for temperatures T=2 MeV (dashed line), 4 MeV (thin solid line, circle symbols), and 6 MeV (dotted line). The stars (thick solid line) are the direct calculation of $\Delta E_{\rm bh}$ according to the adopted hyper-mass formula (2)–(7) at T=0. The initial parameter of the hyper-nuclear system are as in Fig. 1.

statistical process. As was previously established in multifragmentation studies [41, 42], the selection of adequate reaction conditions can be experimentally verified.

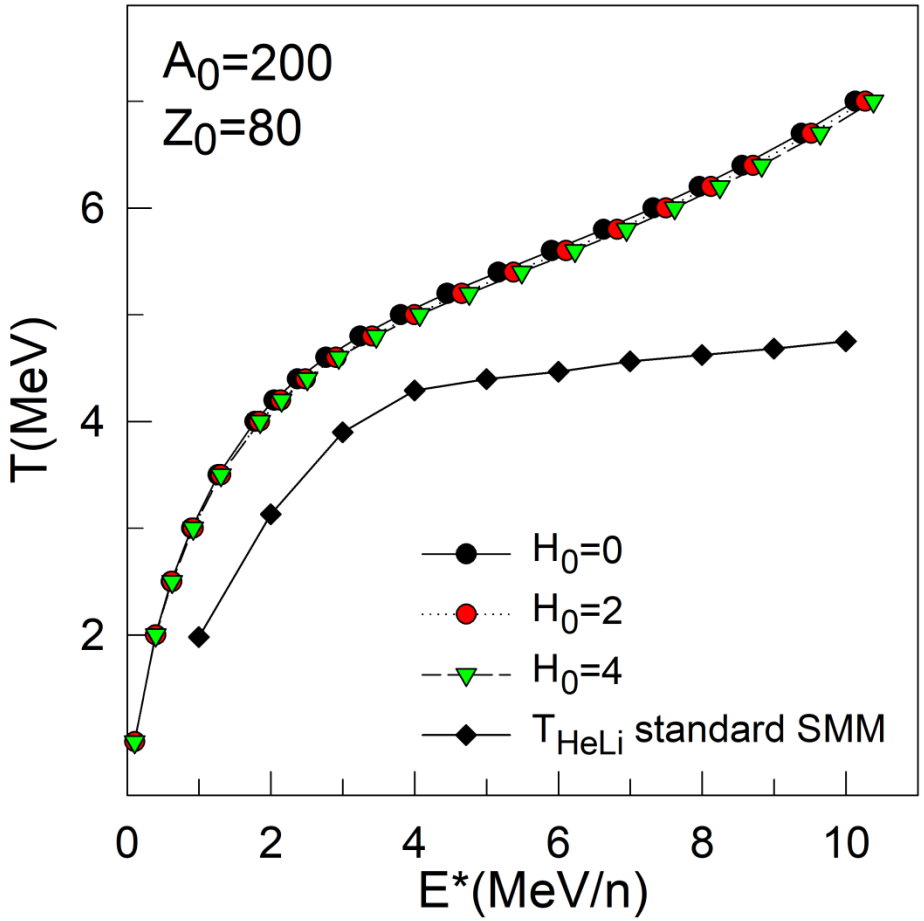

FIG. 3: (Color online) The caloric curve (the temperature versus the excitation energy) for the disintegration of the hyper-nuclear system with parameters given in the figure. The statistical calculations including different initial numbers of hyperons (0, 2, and 4) are shown by different symbols and lines. (For better view the symbols are shifted slightly along the abscissa axis being at the same E^*.) The helium-lithium isotope temperature (see the text) calculated within the standard multifragmentation model are presented by diamonds.

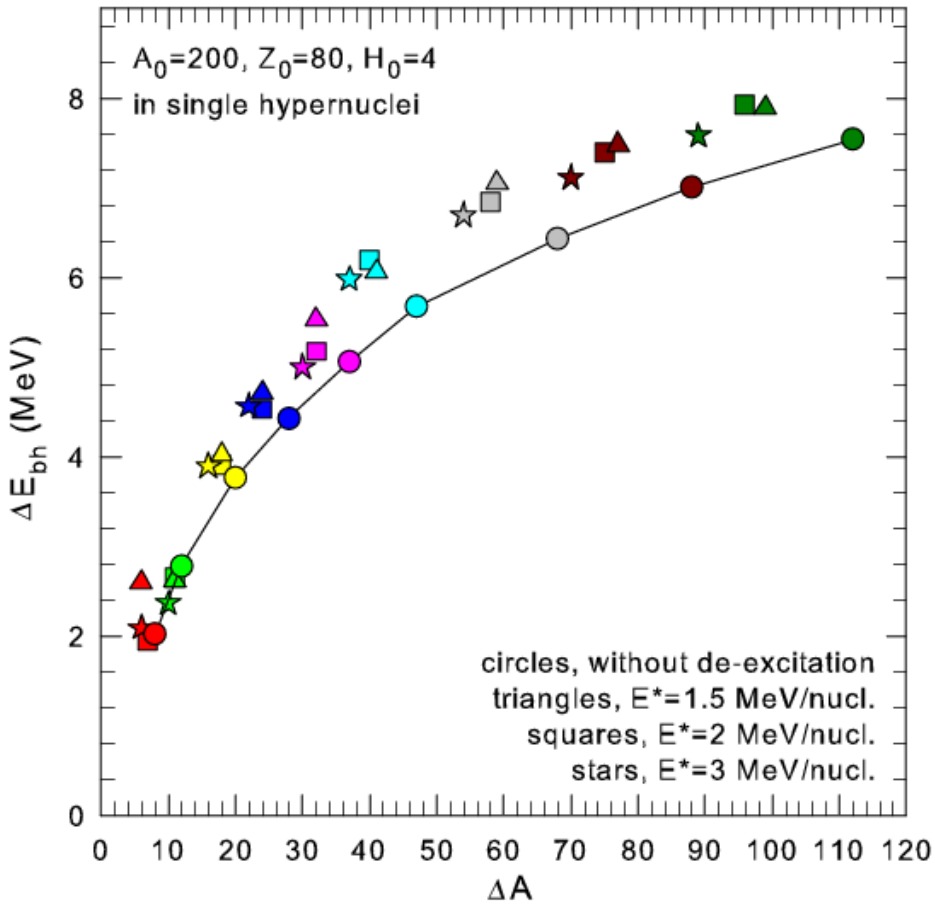

FIG. 4: (Color online) Influence of the secondary de-excitation on the difference of binding energies of hyperons in nuclei $\Delta E_{\rm bh}$ as function of their mass number difference ΔA, by taking single hypernuclei (which are same as in Fig. 2). The calculations of double ratio yields for primary hot nuclei shown for temperature 4 MeV (dashed line, color circle symbols). The triangles, squares, and stars are the calculations with modified double ratios after the secondary de-excitation (via nuclear evaporation) of primary nuclei at excitation energies of 1.5, 2.0, and 3.0 MeV/nucleon, respectively. The same color symbols show the evolution of the $\Delta E_{\rm bh}$ (starting from the circles) corresponding to the nuclei evolution during de-excitation. Other notations as in Fig. 2.

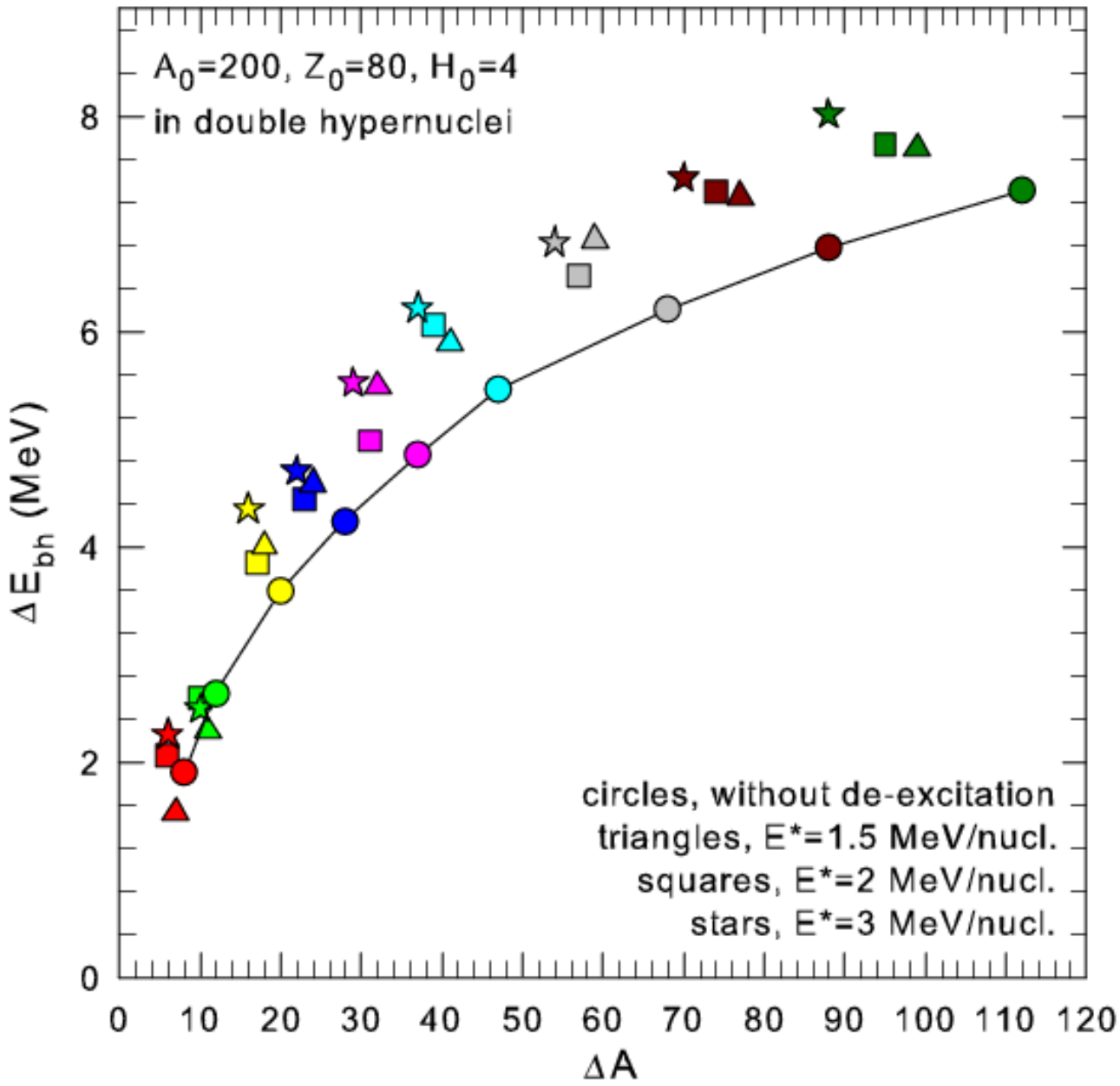

FIG. 5: (Color online) The same as in Fig. 4, however, for double hypernuclei (see the text).

Summary

We have demonstrated that the hyperon binding energies can be effectively evaluated from the yields of different isotopes of hypernuclei.

The double ratio method is suggested for this purpose. The advantage of this procedure is its universality and the possibility to involve many different isotopes. This method can also be applied for multi-strange nuclei, which binding energies were very difficult to measure in previous hypernuclear experiments.

We believe such kind of research would be possible at the new generation of ion accelerators of intermediate energies, as FAIR (Darmstadt), NICA (Dubna), and others.

It is promising that new advanced experimental installations for the fragment detection will be available soon

References

[1] Buyukcizmeci N. et al submitted to Phys. Rev C 2018, (**ArxiV: 1711.01159v2)**

[2] Botvina A.S et al., Phys. Rev. C **94**, 054615 (2016).

[3] Buyukcizmeci N., Botvina A.S., Pochodzalla, J., Bleicher, M., Phys. Rev. C 88, 014611 (2013).

[4]Botvina A.S and Pochodzalla, J., Phys. Rev. C 76, 024909 (2007).

[5]Samanta C, Roy Chowdhury P and Basu D N.,*J. Phys. G: Nucl. Part. Phys.* 32 363(2006).

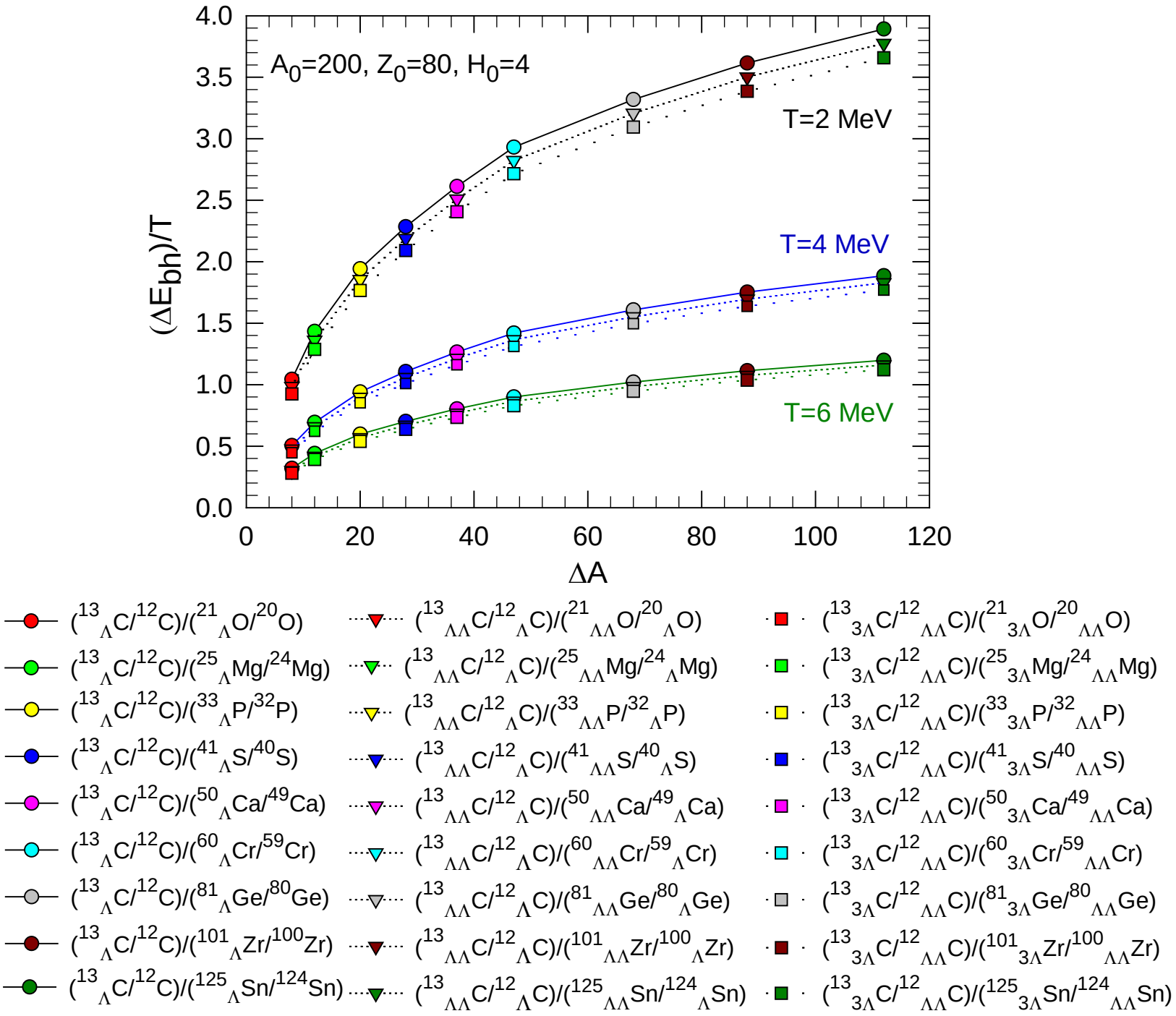
A0=200, Z0=80, H0=4
T=2 MeV
T=4 MeV
T=6 MeV
(ΔEbh)/T
ΔA
0.0
0.5
1.0
1.5
2.0
2.5
3.0
3.5
4.0
0
20
40
60
80
100
120
(13ΛC/12C)/(21ΛO/20O)
(13ΛC/12C)/(25ΛMg/24Mg)
(13ΛC/12C)/(33ΛP/32P)
(13ΛC/12C)/(41ΛS/40S)
(13ΛC/12C)/(50ΛCa/49Ca)
(13ΛC/12C)/(60ΛCr/59Cr)
(13ΛC/12C)/(81ΛGe/80Ge)
(13ΛC/12C)/(101ΛZr/100Zr)
(13ΛC/12C)/(125ΛSn/124Sn)
(13ΛΛC/12ΛC)/(21ΛΛO/20ΛO)
(13ΛΛC/12ΛC)/(25ΛΛMg/24ΛMg)
(13ΛΛC/12ΛC)/(33ΛΛP/32ΛP)
(13ΛΛC/12ΛC)/(41ΛΛS/40ΛS)
(13ΛΛC/12ΛC)/(50ΛΛCa/49ΛCa)
(13ΛΛC/12ΛC)/(60ΛΛCr/59ΛCr)
(13ΛΛC/12ΛC)/(81ΛΛGe/80ΛGe)
(13ΛΛC/12ΛC)/(101ΛΛZr/100ΛZr)
(13ΛΛC/12ΛC)/(125ΛΛSn/124ΛSn)
(13 3ΛC/12 ΛΛC)/(21 3ΛO/20 ΛΛO)
(13 3ΛC/12 ΛΛC)/(25 3ΛMg/24 ΛΛMg)
(13 3ΛC/12 ΛΛC)/(33 3ΛP/32 ΛΛP)
(13 3ΛC/12 ΛΛC)/(41 3ΛS/40 ΛΛS)
(13 3ΛC/12 ΛΛC)/(50 3ΛCa/49 ΛΛCa)
(13 3ΛC/12 ΛΛC)/(60 3ΛCr/59 ΛΛCr)
(13 3ΛC/12 ΛΛC)/(81 3ΛGe/80 ΛΛGe)
(13 3ΛC/12 ΛΛC)/(101 3ΛZr/100 ΛΛZr)
(13 3ΛC/12 ΛΛC)/(125 3ΛSn/124 ΛΛSn)

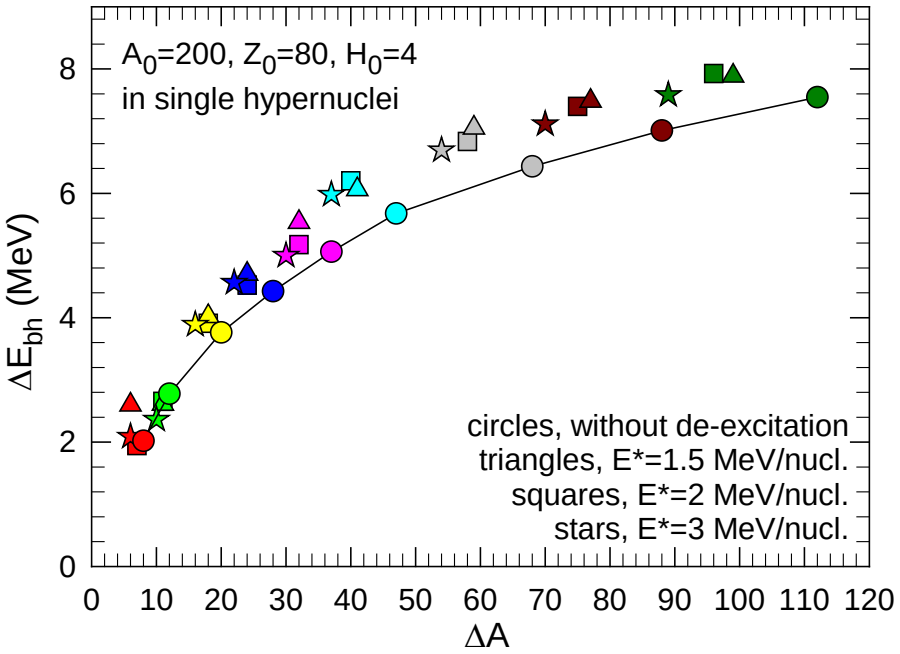

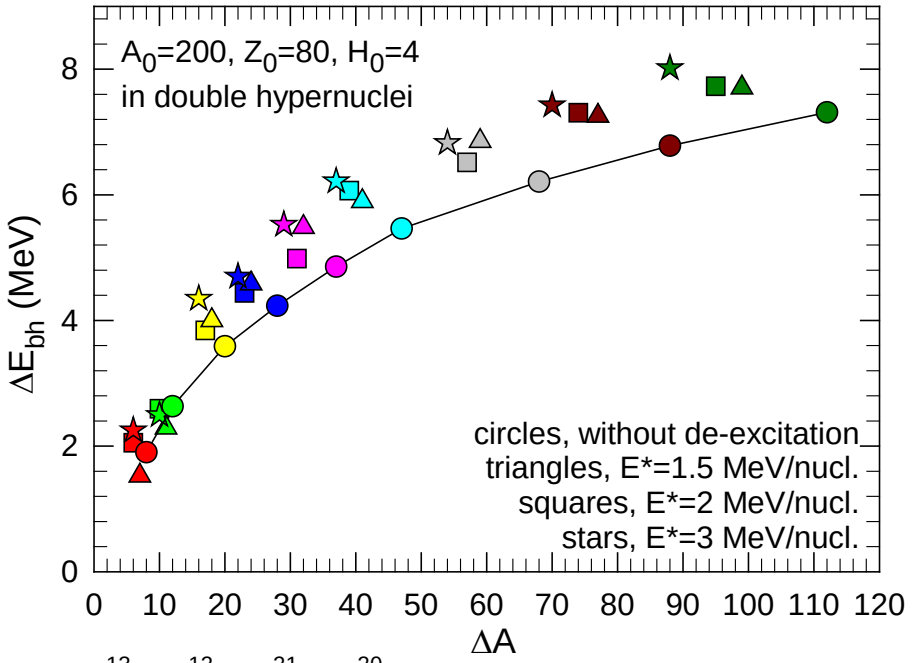

- $(^{13}_{\Lambda}C/^{12}C)/(^{21}_{\Lambda}O/^{20}O)$
- $(^{13}_{\Lambda}C/^{12}C)/(^{25}_{\Lambda}Mg/^{24}Mg)$
- $(^{13}_{\Lambda}C/^{12}C)/(^{33}_{\Lambda}P/^{32}P)$
- $(^{13}_{\Lambda}C/^{12}C)/(^{41}_{\Lambda}S/^{40}S)$
- $(^{13}_{\Lambda}C/^{12}C)/(^{52}_{\Lambda}Ca/^{51}Ca)$
- $(^{13}_{\Lambda}C/^{12}C)/(^{62}_{\Lambda}Cr/^{61}Cr)$
- $(^{13}_{\Lambda}C/^{12}C)/(^{81}_{\Lambda}Ge/^{80}Ge)$
- $(^{13}_{\Lambda}C/^{12}C)/(^{101}_{\Lambda}Zr/^{100}Zr)$
- $(^{13}_{\Lambda}C/^{12}C)/(^{125}_{\Lambda}Sn/^{124}Sn)$
- $(^{12}_{\Lambda}B/^{11}B)/(^{18}_{\Lambda}O/^{17}O)$
- $(^{12}_{\Lambda}B/^{11}B)/(^{23}_{\Lambda}Na/^{22}Na)$
- $(^{12}_{\Lambda}B/^{11}B)/(^{30}_{\Lambda}Si/^{29}Si)$
- $(^{12}_{\Lambda}B/^{11}B)/(^{36}_{\Lambda}S/^{35}S)$
- $(^{12}_{\Lambda}B/^{11}B)/(^{44}_{\Lambda}Ca/^{43}Ca)$
- $(^{12}_{\Lambda}B/^{11}B)/(^{53}_{\Lambda}Cr/^{52}Cr)$
- $(^{12}_{\Lambda}B/^{11}B)/(^{71}_{\Lambda}Ge/^{70}Ge)$
- $(^{12}_{\Lambda}B/^{11}B)/(^{89}_{\Lambda}Zr/^{88}Zr)$
- $(^{12}_{\Lambda}B/^{11}B)/(^{111}_{\Lambda}Sn/^{110}Sn)$
- $(^{11}_{\Lambda}B/^{10}B)/(^{18}_{\Lambda}O/^{17}O)$
- $(^{11}_{\Lambda}B/^{10}B)/(^{22}_{\Lambda}Ne/^{21}Ne)$
- $(^{11}_{\Lambda}B/^{10}B)/(^{29}_{\Lambda}Si/^{28}Si)$
- $(^{11}_{\Lambda}B/^{10}B)/(^{35}_{\Lambda}S/^{34}S)$
- $(^{11}_{\Lambda}B/^{10}B)/(^{43}_{\Lambda}Ca/^{42}Ca)$
- $(^{11}_{\Lambda}B/^{10}B)/(^{51}_{\Lambda}Cr/^{50}Cr)$
- $(^{11}_{\Lambda}B/^{10}B)/(^{69}_{\Lambda}Ge/^{68}Ge)$
- $(^{11}_{\Lambda}B/^{10}B)/(^{86}_{\Lambda}Y/^{85}Y)$
- $(^{11}_{\Lambda}B/^{10}B)/(^{107}_{\Lambda}In/^{106}In)$
- $(^{11}_{\Lambda}B/^{10}B)/(^{17}_{\Lambda}O/^{16}O)$
- $(^{11}_{\Lambda}B/^{10}B)/(^{21}_{\Lambda}Ne/^{20}Ne)$
- $(^{11}_{\Lambda}B/^{10}B)/(^{27}_{\Lambda}Al/^{26}Al)$
- $(^{11}_{\Lambda}B/^{10}B)/(^{33}_{\Lambda}P/^{32}P)$
- $(^{11}_{\Lambda}B/^{10}B)/(^{41}_{\Lambda}K/^{40}K)$
- $(^{11}_{\Lambda}B/^{10}B)/(^{48}_{\Lambda}Ti/^{47}Ti)$
- $(^{11}_{\Lambda}B/^{10}B)/(^{65}_{\Lambda}Zn/^{64}Zn)$
- $(^{11}_{\Lambda}B/^{10}B)/(^{81}_{\Lambda}Rb/^{80}Rb)$
- $(^{11}_{\Lambda}B/^{10}B)/(^{100}_{\Lambda}Pd/^{99}Pd)$

- $(^{13}_{\Lambda\Lambda}C/^{12}_{\Lambda}C)/(^{21}_{\Lambda\Lambda}O/^{20}_{\Lambda}O)$
- $(^{13}_{\Lambda\Lambda}C/^{12}_{\Lambda}C)/(^{25}_{\Lambda\Lambda}Mg/^{24}_{\Lambda}Mg)$
- $(^{13}_{\Lambda\Lambda}C/^{12}_{\Lambda}C)/(^{33}_{\Lambda\Lambda}P/^{32}_{\Lambda}P)$
- $(^{13}_{\Lambda\Lambda}C/^{12}_{\Lambda}C)/(^{41}_{\Lambda\Lambda}S/^{40}_{\Lambda}S)$
- $(^{13}_{\Lambda\Lambda}C/^{12}_{\Lambda}C)/(^{52}_{\Lambda\Lambda}Ca/^{51}_{\Lambda}Ca)$
- $(^{13}_{\Lambda\Lambda}C/^{12}_{\Lambda}C)/(^{62}_{\Lambda\Lambda}Cr/^{61}_{\Lambda}Cr)$
- $(^{13}_{\Lambda\Lambda}C/^{12}_{\Lambda}C)/(^{81}_{\Lambda\Lambda}Ge/^{80}_{\Lambda}Ge)$
- $(^{13}_{\Lambda\Lambda}C/^{12}_{\Lambda}C)/(^{101}_{\Lambda\Lambda}Zr/^{100}_{\Lambda}Zr)$
- $(^{13}_{\Lambda\Lambda}C/^{12}_{\Lambda}C)/(^{125}_{\Lambda\Lambda}Sn/^{124}_{\Lambda}Sn)$
- $(^{12}_{\Lambda\Lambda}B/^{11}_{\Lambda}B)/(^{19}_{\Lambda\Lambda}O/^{18}_{\Lambda}O)$
- $(^{12}_{\Lambda\Lambda}B/^{11}_{\Lambda}B)/(^{23}_{\Lambda\Lambda}Ne/^{22}_{\Lambda}Ne)$
- $(^{12}_{\Lambda\Lambda}B/^{11}_{\Lambda}B)/(^{30}_{\Lambda\Lambda}Si/^{29}_{\Lambda}Si)$
- $(^{12}_{\Lambda\Lambda}B/^{11}_{\Lambda}B)/(^{36}_{\Lambda\Lambda}S/^{35}_{\Lambda}S)$
- $(^{12}_{\Lambda\Lambda}B/^{11}_{\Lambda}B)/(^{44}_{\Lambda\Lambda}Ca/^{43}_{\Lambda}Ca)$
- $(^{12}_{\Lambda\Lambda}B/^{11}_{\Lambda}B)/(^{53}_{\Lambda\Lambda}Cr/^{52}_{\Lambda}Cr)$
- $(^{12}_{\Lambda\Lambda}B/^{11}_{\Lambda}B)/(^{71}_{\Lambda\Lambda}Ge/^{70}_{\Lambda}Ge)$
- $(^{12}_{\Lambda\Lambda}B/^{12}_{\Lambda}B)/(^{89}_{\Lambda\Lambda}Zr/^{88}_{\Lambda}Zr)$
- $(^{12}_{\Lambda\Lambda}B/^{11}_{\Lambda}B)/(^{111}_{\Lambda\Lambda}Sn/^{110}_{\Lambda}Sn)$
- $(^{12}_{\Lambda\Lambda}B/^{11}_{\Lambda}B)/(^{18}_{\Lambda\Lambda}O/^{17}_{\Lambda}O)$
- $(^{12}_{\Lambda\Lambda}B/^{11}_{\Lambda}B)/(^{22}_{\Lambda\Lambda}Ne/^{21}_{\Lambda}Ne)$
- $(^{12}_{\Lambda\Lambda}B/^{11}_{\Lambda}B)/(^{29}_{\Lambda\Lambda}Al/^{28}_{\Lambda}Al)$
- $(^{12}_{\Lambda\Lambda}B/^{11}_{\Lambda}B)/(^{35}_{\Lambda\Lambda}S/^{34}_{\Lambda}S)$
- $(^{12}_{\Lambda\Lambda}B/^{11}_{\Lambda}B)/(^{43}_{\Lambda\Lambda}K/^{42}_{\Lambda}K)$
- $(^{12}_{\Lambda\Lambda}B/^{11}_{\Lambda}B)/(^{51}_{\Lambda\Lambda}V/^{50}_{\Lambda}V)$
- $(^{12}_{\Lambda\Lambda}B/^{11}_{\Lambda}B)/(^{69}_{\Lambda\Lambda}Ga/^{68}_{\Lambda}Ga)$
- $(^{12}_{\Lambda\Lambda}B/^{11}_{\Lambda}B)/(^{86}_{\Lambda\Lambda}Y/^{85}_{\Lambda}Y)$
- $(^{12}_{\Lambda\Lambda}B/^{11}_{\Lambda}B)/(^{107}_{\Lambda\Lambda}Cd/^{106}_{\Lambda}Cd)$
- $(^{11}_{\Lambda\Lambda}B/^{10}_{\Lambda}B)/(^{17}_{\Lambda\Lambda}N/^{16}_{\Lambda}N)$
- $(^{11}_{\Lambda\Lambda}B/^{10}_{\Lambda}B)/(^{21}_{\Lambda\Lambda}F/^{20}_{\Lambda}F)$
- $(^{11}_{\Lambda\Lambda}B/^{10}_{\Lambda}B))/(^{27}_{\Lambda\Lambda}Mg/^{26}_{\Lambda}Mg)$
- $(^{11}_{\Lambda\Lambda}B/^{10}_{\Lambda}B)/(^{33}_{\Lambda\Lambda}P/^{32}_{\Lambda}P)$
- $(^{11}_{\Lambda\Lambda}B/^{10}_{\Lambda}B)/(^{40}_{\Lambda\Lambda}Ar/^{39}_{\Lambda}Ar)$
- $(^{11}_{\Lambda\Lambda}B/^{10}_{\Lambda}B)/(^{48}_{\Lambda\Lambda}Ti/^{47}_{\Lambda}Ti)$
- $(^{11}_{\Lambda\Lambda}B/^{10}_{\Lambda}B)/(^{65}_{\Lambda\Lambda}Zn/^{64}_{\Lambda}Zn)$
- $(^{11}_{\Lambda\Lambda}B/^{10}_{\Lambda}B)/(^{81}_{\Lambda\Lambda}Rb/^{80}_{\Lambda}Rb)$
- $(^{11}_{\Lambda\Lambda}B/^{10}_{\Lambda}B)/(^{99}_{\Lambda\Lambda}Rh/^{98}_{\Lambda}Rh)$

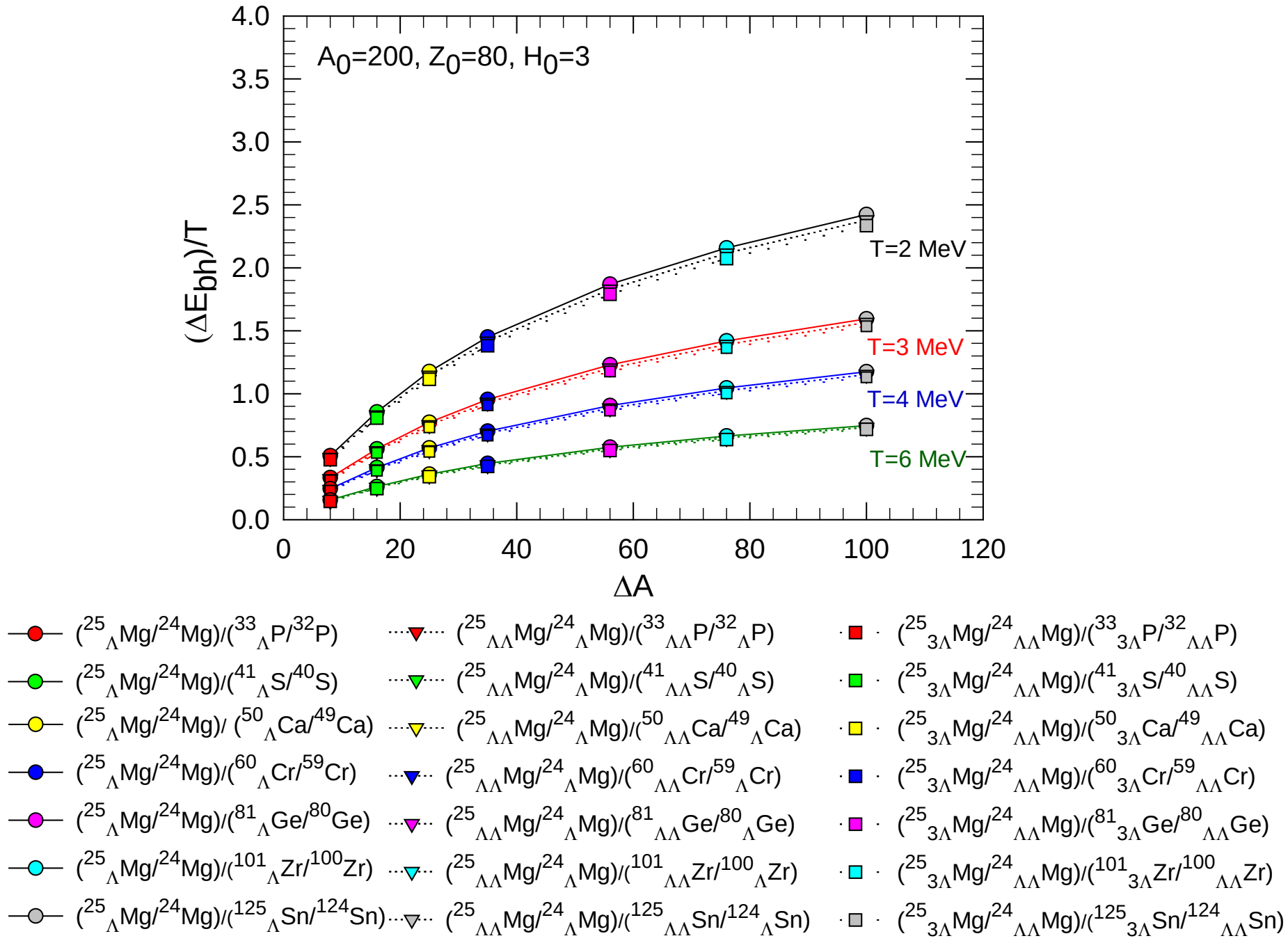
A0=200, Z0=80, H0=3
(ΔEbh)/T
ΔA
T=2 MeV
T=3 MeV
T=4 MeV
T=6 MeV
0.0
0.5
1.0
1.5
2.0
2.5
3.0
3.5
4.0
0
20
40
60
80
100
120
(25ΛMg/24Mg)/(33ΛP/32P)
(25ΛMg/24Mg)/(41ΛS/40S)
(25ΛMg/24Mg)/ (50ΛCa/49Ca)
(25ΛMg/24Mg)/(60ΛCr/59Cr)
(25ΛMg/24Mg)/(81ΛGe/80Ge)
(25ΛMg/24Mg)/(101ΛZr/100Zr)
(25ΛMg/24Mg)/(125ΛSn/124Sn)
(25ΛΛMg/24ΛMg)/(33ΛΛP/32ΛP)
(25ΛΛMg/24ΛMg)/(41ΛΛS/40ΛS)
(25ΛΛMg/24ΛMg)/(50ΛΛCa/49ΛCa)
(25ΛΛMg/24ΛMg)/(60ΛΛCr/59ΛCr)
(25ΛΛMg/24ΛMg)/(81ΛΛGe/80ΛGe)
(25ΛΛMg/24ΛMg)/(101ΛΛZr/100ΛZr)
(25ΛΛMg/24ΛMg)/(125ΛΛSn/124ΛSn)
(25 3ΛMg/24ΛΛMg)/(33 3ΛP/32ΛΛP)
(25 3ΛMg/24ΛΛMg)/(41 3ΛS/40ΛΛS)
(25 3ΛMg/24ΛΛMg)/(50 3ΛCa/49ΛΛCa)
(25 3ΛMg/24ΛΛMg)/(60 3ΛCr/59ΛΛCr)
(25 3ΛMg/24ΛΛMg)/(81 3ΛGe/80ΛΛGe)
(25 3ΛMg/24ΛΛMg)/(101 3ΛZr/100ΛΛZr)
(25 3ΛMg/24ΛΛMg)/(125 3ΛSn/124ΛΛSn)

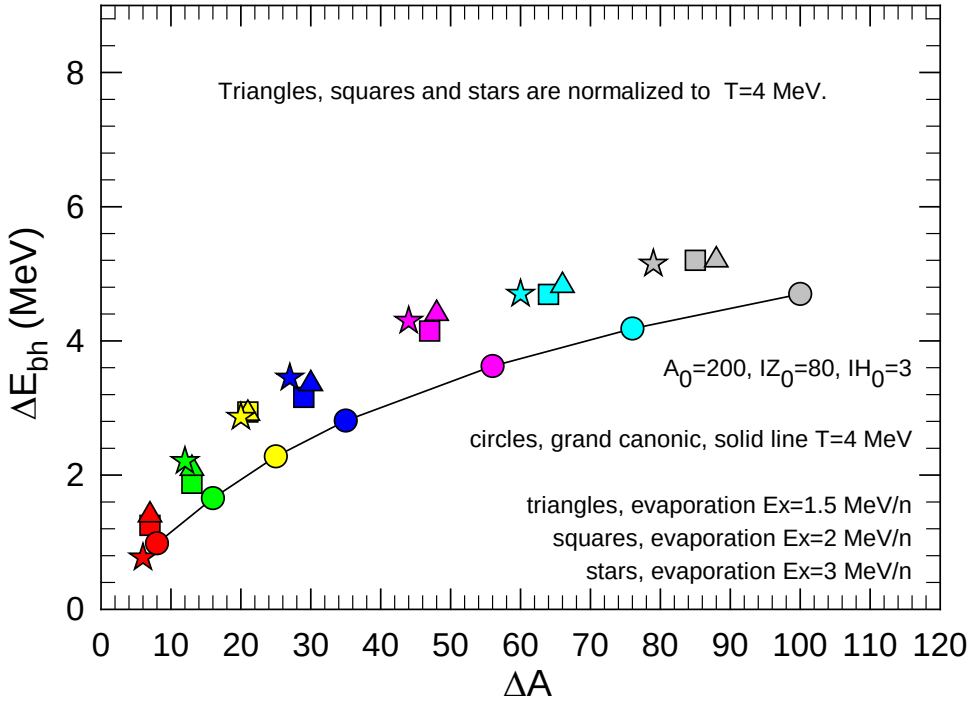

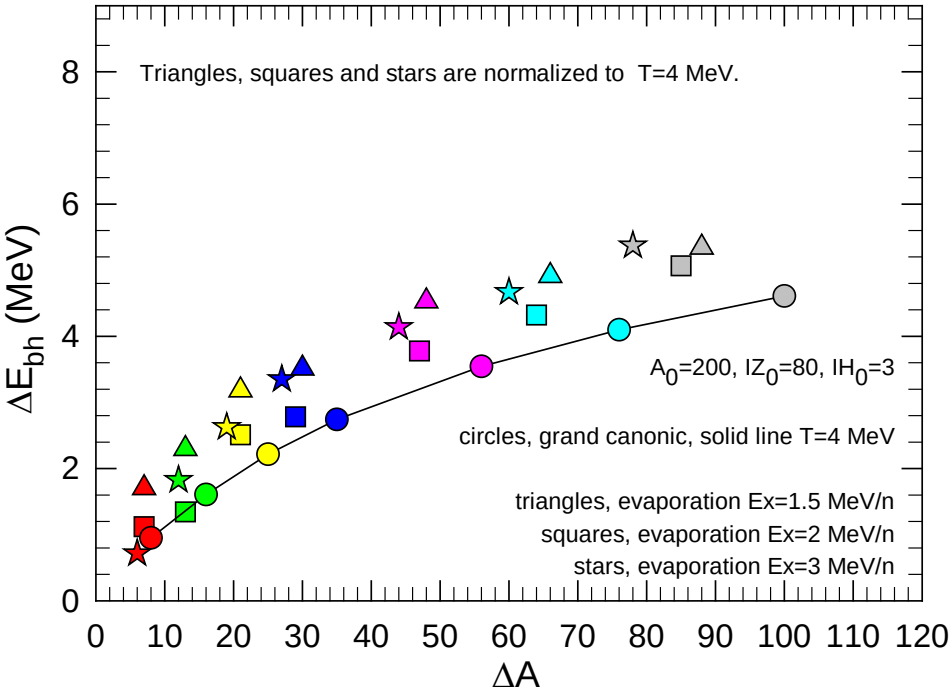

- $(^{25}_{\Lambda}Mg/^{24}Mg)/(^{33}_{\Lambda}P/^{32}P)$
- $(^{25}_{\Lambda}Mg/^{24}Mg/)/(^{41}_{\Lambda}S/^{40}S)$
- $(^{25}_{\Lambda}Mg/^{24}Mg)/(^{50}_{\Lambda}Ca/^{49}Ca)$
- $(^{25}_{\Lambda}Mg/^{24}Mg)/(^{60}_{\Lambda}Cr/^{59}Cr)$
- $(^{25}_{\Lambda}Mg/^{24}Mg)/(^{81}_{\Lambda}Ge/^{80}Ge)$
- $(^{25}_{\Lambda}Mg/^{24}Mg)/(^{101}_{\Lambda}Zr/^{100}Zr)$
- $(^{25}_{\Lambda}Mg/^{24}Mg)/(^{125}_{\Lambda}Sn/^{124}Sn)$
- $(^{23}_{\Lambda}Na/^{22}Na)/(^{30}_{\Lambda}Si/^{29}Si)$
- $(^{23}_{\Lambda}Na/^{22}Na)/(^{36}_{\Lambda}S/^{35}S)$
- $(^{23}_{\Lambda}Na/^{22}Na)/(^{44}_{\Lambda}Ca/^{43}Ca)$
- $(^{23}_{\Lambda}Na/^{22}Na)/(^{53}_{\Lambda}Cr/^{52}Cr)$
- $(^{23}_{\Lambda}Na/^{22}Na)/(^{71}_{\Lambda}Ge/^{70}Ge)$
- $(^{23}_{\Lambda}Na/^{22}Na)/(^{89}_{\Lambda}Zr/^{88}Zr)$
- $(^{23}_{\Lambda}Na/^{22}Na)/(^{111}_{\Lambda}Sn/^{110}Sn)$
- $(^{22}_{\Lambda}Ne/^{21}Ne)/(^{29}_{\Lambda}Si/^{28}Si)$
- $(^{22}_{\Lambda}Ne/^{21}Ne)/(^{35}_{\Lambda}S/^{34}S)$
- $(^{22}_{\Lambda}Ne/^{21}Ne)/(^{43}_{\Lambda}Ca/^{42}Ca)$
- $(^{22}_{\Lambda}Ne/^{21}Ne)/(^{51}_{\Lambda}Cr/^{50}Cr)$
- $(^{22}_{\Lambda}Ne/^{21}Ne)/(^{69}_{\Lambda}Ge/^{68}Ge)$
- $(^{22}_{\Lambda}Ne/^{21}Ne)/(^{86}_{\Lambda}Y/^{85}Y)$
- $(^{22}_{\Lambda}Ne/^{21}Ne)/(^{107}_{\Lambda}In/^{106}In)$
- $(^{21}_{\Lambda}Ne/^{20}Ne)/(^{27}_{\Lambda}Al/^{26}Al)$
- $(^{21}_{\Lambda}Ne/^{20}Ne)/(^{33}_{\Lambda}P/^{32}P)$
- $(^{21}_{\Lambda}Ne/^{20}Ne)/(^{41}_{\Lambda}K/^{40}K)$
- $(^{21}_{\Lambda}Ne/^{20}Ne)/(^{48}_{\Lambda}Ti/^{47}Ti)$
- $(^{21}_{\Lambda}Ne/^{20}Ne)/(^{65}_{\Lambda}Zn/^{64}Zn)$
- $(^{21}_{\Lambda}Ne/^{20}Ne)/(^{81}_{\Lambda}Rb/^{80}Rb)$
- $(^{21}_{\Lambda}Ne/^{20}Ne)/(^{100}_{\Lambda}Pd/^{99}Pd)$

- $(^{25}_{\Lambda\Lambda}Mg/^{24}_{\Lambda}Mg)/(^{33}_{\Lambda\Lambda}P/^{32}_{\Lambda}P)$
- $(^{25}_{\Lambda\Lambda}Mg/^{24}_{\Lambda}Mg)/(^{41}_{\Lambda\Lambda}S/^{40}_{\Lambda}S)$
- $(^{25}_{\Lambda\Lambda}Mg/^{24}_{\Lambda}Mg)/(^{52}_{\Lambda\Lambda}Ca/^{51}_{\Lambda}Ca)$
- $(^{25}_{\Lambda\Lambda}Mg/^{24}_{\Lambda}Mg)/(^{62}_{\Lambda\Lambda}Cr/^{61}_{\Lambda}Cr)$
- $(^{25}_{\Lambda\Lambda}Mg/^{24}_{\Lambda}Mg)/(^{81}_{\Lambda\Lambda}Ge/^{80}_{\Lambda}Ge)$
- $(^{25}_{\Lambda\Lambda}Mg/^{24}_{\Lambda}Mg)/(^{101}_{\Lambda\Lambda}Zr/^{100}_{\Lambda}Zr)$
- $(^{25}_{\Lambda\Lambda}Mg/^{24}_{\Lambda}Mg)/(^{125}_{\Lambda\Lambda}Sn/^{124}_{\Lambda}Sn)$
- $(^{23}_{\Lambda\Lambda}Ne/^{22}_{\Lambda}Ne)/(^{30}_{\Lambda\Lambda}Si/^{29}_{\Lambda}Si)$
- $(^{23}_{\Lambda\Lambda}Ne/^{22}_{\Lambda}Ne)/(^{36}_{\Lambda\Lambda}S/^{35}_{\Lambda}S)$
- $(^{23}_{\Lambda\Lambda}Ne/^{22}_{\Lambda}Ne)/(^{44}_{\Lambda\Lambda}Ca/^{43}_{\Lambda}Ca)$
- $(^{23}_{\Lambda\Lambda}Ne/^{22}_{\Lambda}Ne)/(^{53}_{\Lambda\Lambda}Cr/^{52}_{\Lambda}Cr)$
- $(^{23}_{\Lambda\Lambda}Ne/^{22}_{\Lambda}Ne)/(^{71}_{\Lambda\Lambda}Ge/^{70}_{\Lambda}Ge)$
- $(^{23}_{\Lambda\Lambda}Ne/^{22}_{\Lambda}Ne)/(^{89}_{\Lambda\Lambda}Zr/^{88}_{\Lambda}Zr)$
- $(^{23}_{\Lambda\Lambda}Ne/^{22}_{\Lambda}Ne)/(^{111}_{\Lambda\Lambda}Sn/^{110}_{\Lambda}Sn)$
- $(^{22}_{\Lambda\Lambda}Ne/^{21}_{\Lambda}Ne)/(^{29}_{\Lambda\Lambda}Al/^{28}_{\Lambda}Al)$
- $(^{22}_{\Lambda\Lambda}Ne/^{21}_{\Lambda}Ne)/(^{35}_{\Lambda\Lambda}S/^{34}_{\Lambda}S)$
- $(^{22}_{\Lambda\Lambda}Ne/^{21}_{\Lambda}Ne)/(^{43}_{\Lambda\Lambda}K/^{42}_{\Lambda}K)$
- $(^{22}_{\Lambda\Lambda}Ne/^{21}_{\Lambda}Ne)/(^{51}_{\Lambda\Lambda}V/^{50}_{\Lambda}V)$
- $(^{22}_{\Lambda\Lambda}Ne/^{21}_{\Lambda}Ne)/(^{69}_{\Lambda\Lambda}Ga/^{68}_{\Lambda}Ga)$
- $(^{22}_{\Lambda\Lambda}Ne/^{21}_{\Lambda}Ne)/(^{86}_{\Lambda\Lambda}Y/^{85}_{\Lambda}Y)$
- $(^{22}_{\Lambda\Lambda}Ne/^{21}_{\Lambda}Ne)/(^{107}_{\Lambda\Lambda}Cd/^{106}_{\Lambda}Cd)$
- $(^{21}_{\Lambda\Lambda}F/^{20}_{\Lambda}F)/(^{27}_{\Lambda\Lambda}Mg/^{26}_{\Lambda}Mg)$
- $(^{21}_{\Lambda\Lambda}F/^{20}_{\Lambda}F)/(^{33}_{\Lambda\Lambda}P/^{32}_{\Lambda}P)$
- $(^{21}_{\Lambda\Lambda}F/^{20}_{\Lambda}F)/(^{40}_{\Lambda\Lambda}Ar/^{39}_{\Lambda}Ar)$
- $(^{21}_{\Lambda\Lambda}F/^{20}_{\Lambda}F)/(^{48}_{\Lambda\Lambda}Ti/^{47}_{\Lambda}Ti)$
- $(^{21}_{\Lambda\Lambda}F/^{20}_{\Lambda}F)(^{65}_{\Lambda\Lambda}Zn/^{64}_{\Lambda}Zn)$
- $(^{21}_{\Lambda\Lambda}F/^{20}_{\Lambda}F)/(^{81}_{\Lambda\Lambda}Rb/^{80}_{\Lambda}Rb)$
- $(^{21}_{\Lambda\Lambda}F/^{20}_{\Lambda}F)/(^{99}_{\Lambda\Lambda}Rh/^{98}_{\Lambda}Rh)$

Comparison of liquid drop and Samanta formula integrated with hyper-SMM

- Both formula have the similar trend except the intermediate mass fragments